Biochemical Pharmacology 190 (2021) 114590

Contents lists available at ScienceDirect

Biochemical Pharmacology

journal homepage: www.elsevier.com/locate/biochempharm

A comprehensive time course and correlation analysis of indomethacin-induced inflammation, bile acid alterations and dysbiosis in the rat small intestine

Bernadette Lázár [a], Szilvia B. László [a], Barbara Hutka [a], András S. Tóth [a], Amir Mohammadzadeh [a], Eszter Berekméri [a,b], Bence Ágg [a,c], Mihály Balogh [a], Viktor Sajtos [a], Kornél Király [a], Mahmoud Al-Khrasani [a], Anna Földes [d], Gábor Varga [d], Nóra Makra [e], Eszter Ostorházi [e], Dóra Szabó [e], Balázs Ligeti [f], Ágnes Kemény [g,h], Zsuzsanna Helyes [h], Péter Ferdinandy [a,c], Klára Gyires [a], Zoltán S. Zádori [a,*]

[a] Department of Pharmacology and Pharmacotherapy, Semmelweis University, 1089 Budapest, Hungary
[b] Department of Ecology, University of Veterinary Medicine, 1078 Budapest, Hungary
[c] Pharmahungary Group, 6722 Szeged, Hungary
[d] Department of Oral Biology, Semmelweis University, 1089 Budapest, Hungary
[e] Department of Medical Microbiology, Semmelweis University, 1089 Budapest, Hungary
[f] Faculty of Information Technology and Bionics, Pázmány Péter Catholic University, 1083 Budapest, Hungary
[g] Department of Medical Biology, University of Pécs, 7624 Pécs, Hungary
[h] Department of Pharmacology and Pharmacotherapy, Medical School & Szentágothai Research Centre, University of Pécs, 7624 Pécs, Hungary

ARTICLE INFO

Keywords:
Nonsteroidal anti-inflammatory drug
Enteropathy
Inflammation
Bile acid
Microbiota
Correlation

ABSTRACT

It has been proposed that changes in microbiota due to nonsteroidal anti-inflammatory drugs (NSAIDs) alter the composition of bile, and elevation of hydrophobic secondary bile acids contributes to small intestinal damage. However, little is known about the effect of NSAIDs on small intestinal bile acids, and whether bile alterations correlate with mucosal injury and dysbiosis. Here we determined the ileal bile acid metabolome and microbiota 24, 48 and 72 h after indomethacin treatment, and their correlation with each other and with tissue damage in rats. In parallel with the development of inflammation, indomethacin increased the ileal proportion of glycine and taurine conjugated bile acids, but not bile hydrophobicity. Firmicutes decreased with time, whereas Gammaproteobacteria increased first, but declined later and were partially replaced by *Bilophila*, *Bacteroides* and *Fusobacterium*. Mucosal injury correlated negatively with unconjugated bile acids and Gram-positive bacteria, and positively with taurine conjugates and some Gram-negative taxa. Strong positive correlation was found between *Lactobacillaceae*, *Ruminococcaceae*, *Clostridiaceae* and unconjugated bile acids. Indomethacin-induced dysbiosis was not likely due to direct antibacterial effects or alterations in luminal pH. Here we provide the first detailed characterization of indomethacin-induced time-dependent alterations in small intestinal bile acid composition, and their associations with mucosal injury and dysbiosis. Our results suggest that increased bile hydrophobicity is not likely to contribute to indomethacin-induced small intestinal damage.

Abbreviations: ASBT, apical sodium-dependent bile acid transporter; CA, cholic acid; CDCA, chenodeoxycholic acid; COX, cyclooxygenase; DCA, deoxycholic acid; FXR, farnesoid X receptor; GCA, glycocholic acid; GCDCA, glycochenodeoxycholic acid; GDCA, glycodeoxycholic acid; GUDCA, glycoursodeoxycholic acid; HDCA, hyodeoxycholic acid; LC-MS/MS, liquid chromatography-tandem mass spectrometry; LCA, lithocholic acid; MCA, muricholic acid; MIC, minimum inhibitory concentration; NSAID, nonsteroidal anti-inflammatory drug; PCA, principal component analysis; TCA, taurocholic acid; TCDCA, taurochenodeoxycholic acid; TDCA, taurodeoxycholic acid; TLCA, taurolithocholic acid; TMCA, tauromuricholic acid; TUDCA, tauroursodeoxycholic acid; UDCA, ursodeoxycholic acid.

* Corresponding author at: Department of Pharmacology and Pharmacotherapy, Semmelweis University, Nagyvárad tér 4., 1089 Budapest, Hungary.
E-mail address: zadori.zoltan@med.semmelweis-univ.hu (Z.S. Zádori).

https://doi.org/10.1016/j.bcp.2021.114590
Received 26 February 2021; Received in revised form 13 April 2021; Accepted 28 April 2021
Available online 1 May 2021

1. Introduction

Nonsteroidal anti-inflammatory drugs (NSAIDs) belong to the most commonly used medications worldwide, being taken by more than 30 million people on a daily basis [1]. Due to their anti-inflammatory and analgesic properties the popularity of these drugs remains undiminished, although their chronic use is associated with significant adverse events. Gastrointestinal (GI) injury is one of the most important side effects of NSAIDs, which is not limited to the stomach and duodenum, but also to the distal small intestine. In fact, small intestinal damage (enteropathy) can occur in up to 70% of chronic NSAID users [2]. However, despite intensive research the complex pathogenesis of NSAID-enteropathy remains insufficiently understood. Several factors are likely to contribute to the mucosal damage, including the enterohepatic recirculation and local damaging (topical) effects of NSAIDs, inhibition of cyclooxygenase (COX)-1-mediated prostaglandin synthesis, and the intestinal bacteria [3–5].

An additional important contributing factor to intestinal injury is the increased cytotoxicity of bile caused by NSAIDs. It has been repeatedly demonstrated that the combination of these drugs and bile are more toxic to epithelial and other cells than either alone [6–9]. One of the proposed underlying mechanisms is the micellar incorporation of NSAIDs resulting in more toxic micelles [6,7,9], but alterations in the bile acid composition may also result in enhanced cytotoxicity. Namely, it was reported that indomethacin increased the biliary proportion of hydrophobic secondary bile acids [10,11]. As cellular toxicity of bile acids increases with hydrophobicity [12], it has been proposed that the elevated concentration of secondary bile acids increases bile hydrophobicity, which may contribute to NSAID-induced intestinal damage [3,10,13].

However, upon entering into the intestinal lumen, bile acids are extensively metabolized by the resident microbiota-derived multiple enzymes, including hydrolases, dehydroxylases, dehydrogenases and epimerases [14]. Hence, the amount of distinct bile acids varies substantially over different compartments of the gastrointestinal tract [15,16]. More importantly, the same treatment can induce different changes in bile acids at different gastrointestinal levels [17]. In a recent publication focusing mainly on the combined toxicity of ibuprofen and glucocorticoids [18], notable differences were reported between the hepatic and ileal bile acid profile of ibuprofen-treated mice. To date, it has not been addressed whether NSAIDs increase the concentration of hydrophobic bile acids in the distal small intestine, and whether this correlates with the severity of mucosal damage.

As intestinal bile acid composition depends largely on the composition of microbiota, an additional important factor that cannot be overlooked is the effect of NSAIDs on intestinal bacteria. It is well-established, that NSAIDs cause dysbiosis in the small and large intestine in rodents [8,19–23], and also in humans [24], which is typically characterized by a decrease in the numbers of Gram-positive bacteria in favor of Gram-negative microorganisms. This dysbiosis may also contribute to the mucosal damage, for example, via activation of Toll-like receptor 4 (TLR4) by Gram-negative bacteria [25]. Since in most studies NSAID-induced dysbiosis was analyzed at a single time point, there are only limited data about the dynamics of microbial alterations. However, the proportion of individual taxa following NSAID treatment may change significantly over time [23]. Therefore, it is reasonable to assume that NSAID-evoked bile acid alterations change over time as well, depending on the actual composition of microbiota and the availability of bacterial enzymes involved in bile acid metabolism. Furthermore, the altered bile acid profile may promote changes in microbiota as well, via multiple, direct and receptor-mediated indirect mechanisms [26,27]. Hence, disturbing the subtle and delicate balance between intestinal bacteria and bile acids with an NSAID may result in dynamic, time-dependent changes of both factors in a complex manner.

In the present study we aimed to determine the time course of small intestinal bile acid alterations caused by indomethacin in a widely used subacute animal model of NSAID-enteropathy, in parallel with the development of mucosal inflammation and changes in microbiota. Furthermore, in order to better understand the interplay between these factors, correlations between the measured inflammatory markers, bile acids and bacterial taxa were calculated. Here we show that indomethacin induced time-dependent changes in ileal bile acid composition, which were mainly characterized by a shift towards a higher proportion of conjugated bile acids. This was accompanied by a gradual loss of bacteria belonging to Firmicutes, whereas Gammaproteobacteria increased first, but declined later and were partially replaced by *Bilophila*, *Bacteroides* and *Fusobacterium*. The development of mucosal damage occured in parallel and correlated positively with the rise in conjugates and Gram-negative bacteria, but not with changes in bile hydrophobicity, which argues against its role in the pathogenesis of NSAID-enteropathy.

2. Materials and methods

2.1. Animals

Experiments were carried out on male Wistar rats weighing 160–180 g (Toxi-Coop Ltd., Budapest, Hungary). Animals were housed in a temperature (22 ± 2 °C)- and humidity-controlled room at a 12-h light/dark cycle. Food and water were available *ad libitum*.

2.2. Ethical considerations

All efforts were made to minimize animal suffering and to reduce the number of animals used in the experiments. All procedures conformed to the Directive 2010/63/EU on European Convention for the protection of animals used for scientific purposes. The experiments were approved by the National Scientific Ethical Committee on Animal Experimentation and permitted by the government (Food Chain Safety and Animal Health Directorate of the Government Office for Pest County (PEI/001/1493-4/2015)).

2.3. Study design and induction of enteropathy

Before the start of the experiment rats were co-housed to homogenize their microbiota, and then randomly allocated into 4 experimental groups, with 10 rats in each group. Thereafter, the rats of all groups were further divided and housed in 2–2 individually ventillated cages, with 5 rats per cage, to minimize the cage effect [28].

Because NSAIDs primarily damage the distal small intestine [3,29], in the present study we focused on the ileal bile acids and microbiota. In order to analyze NSAID-induced bile acid alterations, small intestinal damage and dysbiosis, we used a well-established subacute model of enteropathy [29,30], in which a single, large dose (20 mg/kg) of indomethacin (Sigma, St. Louis, MO, USA) was given to three of the experimental groups, in a volume of 0.33 ml/100 g by oral gavage. Then, the groups were sacrificed at different time points, namely, 24, 48 or 72 h after the indomethacin challenge. Our preliminary experiments showed that the bile acid metabolome and the microbiota composition of vehicle (1% hydroxyethylcellulose)-treated rats are stable over time (data not shown), provided that there are no changes in their environment. Therefore, the rats of the fourth group (control) were sacrificed at a single time point, 72 h after the administration of hydroxyethylcellulose vehicle (Sigma, St. Louis, MO, USA). This also complies with the principle of reduction of animal experiments [31].

At the time of sacrifice, animals were euthanized under CO_2, the small intestines were excised, the content of ileum was quickly collected, snap-frozen in liquid nitrogen and stored at −80 °C for analysis of bile acids, microbial composition and luminal pH. The mucosa of the small intestine was flushed with cold saline and the severity of enteropathy was evaluated by a scoring system adapted from [32], including three parameters: the number of ulcers (from 0: no ulcers to 3: numerous

ulcers throughout the mid and distal small intestine), tissue adhesion (from 0: normal appearance to 3: multiple adhesions, making it difficult to remove the intestine intact) and the extent of ascites (from 0: no ascites to 3: abdominal cavity full of fluid, massive peritonitis). The length of the whole small intestine was also measured, as another parameter to assess intestinal inflammation. Then, full-thickness pieces of the ileum, as well as liver samples were snap-frozen in liquid nitrogen, pulverized and stored at −80 °C for further analyses. A further ileal segment was fixed in 10% formalin for evaluation of microscopic damage.

2.4. Measurement of myeloperoxidase and inflammatory cytokines

Milliplex MAP assay based on the Luminex xMAP technology was performed to determine the small intestinal protein concentrations of interleukin-1β (IL-1β) and interleukin-10 (IL-10), by using customized Milliplex Rat Cytokine/Chemokine Magnetic Bead Panel (Merck Millipore, Burlington, USA), whereas ELISA kits were used to quantify the protein levels of tumor necrosis factor-α (TNF-α) (Invitrogen, Camirillo, CA) and myeloperoxidase (MPO) (Hycult Biotech, Uden, The Netherlands). Tissue samples were homogenized and assayed according to the manufacturers' instructions, in a blind fashion and in duplicates. The total protein concentration of supernatants was determined by using a bicinchoninic acid assay kit (Thermo Scientific Pierce Protein Research Products, Rockford, USA) with bovine serum albumin as a standard.

2.5. Western blot analysis of cyclooxygenase isoforms and claudin-1

Western blot analysis was performed as previously described [33] and all experiments were repeated at least two times. Briefly, small intestinal tissue samples were homogenized with a TissueLyser (Qiagen, Venlo, The Netherlands) in lysis buffer containing 200 mM NaCl, 5 mM EDTA, 10 mM Tris, 10% glycerine, and 1 μg/mL leupeptin (pH 7.4), supplemented with a protease inhibitor cocktail (cOmplete ULTRA Tablets, Roche, Penzberg, Germany) and PMSF (Sigma, St. Louis, MO, USA). The homogenized lysates were centrifuged twice at 1500*g* and 4 °C for 15 min, then the supernatants were collected and their protein concentration was measured by the bicinchoninic acid assay (Thermo Fisher Scientific, Waltham, MA, USA). Equal amount of protein (20 μg) was mixed with Pierce Lane Marker reducing sample buffer (Thermo Fisher Scientific, Waltham, MA, USA), and loaded and separated in a 4–20% precast Tris-glycine SDS polyacrilamide gel (Bio-Rad, Hercules, CA, USA). Proteins were transferred electrophoretically onto a polyvinylidene difluoride membrane (Bio-Rad, Hercules, CA, USA) at 200 mA overnight. Membranes were blocked with 5% nonfat dry milk (Bio-Rad, Hercules, CA, USA) in Tris-buffered saline containing 0.05% Tween-20 (0.05% TBS-T; Sigma, St. Louis, MO, USA) at room temperature for 2 h. Membranes were incubated with primary antibodies against COX-1 (#4841, 1:500, Lot: 4), COX-2 (#12282, 1:500, Lot: 4) (Cell Signaling Technology, Danvers, MA, USA) and claudin-1 (ab15098, 1:1000; Lot: GR3227 658-2) (Abcam, Cambridge, UK) overnight at 4 °C, followed by 2 h incubation at room temperature with anti-rabbit HRP-linked secondary antibody. GAPDH was used to control for sample loading and protein transfer and to normalize the content of target protein. Signals were detected with a chemiluminescence kit (Bio-Rad, Hercules, CA, USA) by Chemidoc XRS+ (Bio-Rad, Hercules, CA, USA).

2.6. Measurement of Asbt, FXR and Cyp7a1 mRNA by qRT-PCR

Total RNA was obtained from 10 to 30 mg of small intestinal and liver tissue using the QIAzol extraction method (Qiagen, Hilden, Germany), then cDNA was synthesized from total RNA by using Sensifast cDNA synthesis kit (Bioline, London, UK) according to the manufacturer's protocol. The transcript levels of the apical sodium-dependent bile acid transporter (ASBT) and farnesoid X receptor (FXR) in the ileum, and of CYP7A1 in the liver were determined by quantitative real-time polymerase chain reaction (qRT-PCR), performed with SensiFAST SYBR® No-ROX kit (Bioline, London, UK) on a Light Cycler® 480 System (Roche, Penzberg, Germany). Expression levels were calculated with the $2^{-\Delta\Delta CT}$ method and RPL13a was used as a reference gene. Primers used for determination had the following sequences: *Asbt* forward TGG GTT TCT TCC TGG CTA GAC T, *Asbt* reverse TGT TCT GCA TTC CAG TTT CCA A (Accession No.: NM_017222.2), *Fxr* forward AGG CCA TGT TCC TTC GTT CA, *Fxr* reverse TTC AGC TCC CCG ACA CTT TT (Accession No.: NM_021745), *Cyp7a1* forward CTG TCA TAC CAC AAA GTC TTA TGT CA, *Cyp7a1* reverse ATG CTT CTG TGT CCA AAT GCC (Accession No.: NM_01942.2), *Rpl13a* forward GGA TCC CTC CAC CCT ATG ACA, *Rpl13a* reverse CTG GTA CTT CCA CCC GAC CTC (NM_173340.2).

2.7. Measurement of small intestinal bile acids by LC-MS/MS

Luminal samples obtained from the distal small intestine were weighed, mixed with the 3-fold volume of extraction buffer (85% ethanol, 15% 0.01 M phosphate buffer (pH 7.4)), and vortexed thoroughly until dissolution. Samples were then and centrifuged, and the supernatant was used for further analysis. A highly selective reversed phase high-performance liquid chromatography-tandem mass spectrometry (LC-MS/MS) analysis method in negative ion multiple reaction monitoring detection mode was applied to determine the concentrations of 20 different bile acids (Table 1), by using the Biocrates® Bile Acids Kit (Biocrates Life Science AG, Innsbruck, Austria). The samples were extracted via dried filter spot technique in 96-well plate format. Sample extracts were measured by LC-ESI-MS/MS with a SCIEX 4000 QTRAP® (SCIEX, Darmstadt, Germany) instrument. For highly accurate quantification, 7-point external calibration curves and 10 stable isotope-labeled internal standards were applied. Data of bile acids were quantified using the appropriate MS software (SCIEX – Analyst) and the results were finally imported into Biocrates MetIDQ software for further analysis.

The mean hydrophobicity index of the luminal content was calculated as a percentage-weighted mean of previously reported hydrophobicities of the individual bile acids [34–36].

2.8. Antibacterial activity assay

The antibacterial activities of indomethacin and various antibiotics (used as positive controls) were evaluated on a panel of Gram-positive and Gram-negative bacteria with the broth microdilution method according to the EUCAST guideline (www.eucast.org), as previously described [37]. Bacterial strains were grown on COS agar (Columbia agar + 5% sheep blood, Biomérieux, Budapest, Hungary) at 35.5 °C

Table 1
The list of measured bile acids.

Abbreviation	Name	Type
CA	Cholic acid	Primary
CDCA	Chenodeoxycholic acid	Primary
DCA	Deoxycholic acid	Secondary
GCA	Glycocholic acid	Primary, glycine-conjugated
GCDCA	Glycochenodeoxycholic acid	Primary, glycine-conjugated
GDCA	Glycodeoxycholic acid	Secondary, glycine-conjugated
GUDCA	Glycoursodeoxycholic acid	Secondary, glycine-conjugated
HDCA	Hyodeoxycholic acid	Secondary
LCA	Lithocholic acid	Secondary
MCA(α)	α-Muricholic acid	Primary
MCA(β)	β-Muricholic acid	Primary
MCA(ω)	ω-Muricholic acid	Secondary
TCA	Taurocholic acid	Primary, taurine-conjugated
TCDCA	Taurochenodeoxycholic acid	Primary, taurine-conjugated
TDCA	Taurodeoxycholic acid	Secondary, taurine-conjugated
TLCA	Taurolithocholic acid	Secondary, taurine-conjugated
TMCA(α + β)	α- & β-Tauromuricholic acid	Primary, taurine-conjugated
TUDCA	Tauroursodeoxycholic acid	Secondary, taurine-conjugated
UDCA	Ursodeoxycholic acid	Secondary

overnight. Appropriate numbers of colonies were suspended in physiological saline in order to reach the density of 0.5 McFarland for inoculation. Stock solutions containing the different substances were prepared with either 100% (indomethacin) or 50% DMSO (all other substances, diluted with distilled water). These were two-fold serially diluted from 256 to 0.5 mg/L in cation-adjusted Mueller-Hinton broth (Biolab, Budapest, Hungary) and 100 μl of each dilution was transferred into microplate holes. Inoculation was carried out with 10 μl of each bacterial suspension. Incubation was performed at 35 °C for 24 h and minimal inhibitory concentrations (MICs) were determined visually.

2.9. DNA isolation, 16S rRNA gene library preparation and MiSeq sequencing

Bacterial DNA was extracted from 100 mg small intestinal content per sample using the QIAamp PowerFecal DNA Kit (Qiagen, Hilden, Germany) and further purified using AMPure XP beads (Beckman Coulter, Brea, CA, USA) according to the manufacturer's protocols. The concentration of genomic DNA was measured using a Qubit 2.0 Fluorometer with Qubit dsDNA HS Assay Kit (Thermo Fisher Scientific, Waltham, MA, USA). Bacterial DNA was amplified with tagged primers (5′-TCG TCG GCA GCG TCA GAT GTG TAT AAG AGA CAG CCT ACG GGN GGC WGC AG and 5′-GTC TCG TGG GCT CGG AGA TGT GTA TAA GAG ACA GGA CTA CHV GGG TAT CTA ATC C), covering the V3-V4 region of the bacterial 16S rRNA gene. PCR and DNA purifications were performed according to Illumina's demonstrated protocol (Part # 15044223 Rev. B). The PCR product libraries were quantified and qualified by using DNA 1000 Kit on Agilent 2100 Bioanalyzer instrument (Agilent Technologies, Waldbronn, Germany). Equimolar concentrations of libraries were pooled and sequenced on an Illumina MiSeq platform (Illumina, San Diego, CA, USA) using MiSeq Reagent Kit v3 (600 cycles PE).

Essentially the bioinformatic analysis was carried out as described by Mansour et al. [38]. Briefly, the quality of raw reads was assed with FastQC and MultiQC [39], the low quality sequences were filtered and trimmed by Trimmomatic [40] and only sequences with minimal length of 36 were kept, and the low quality base calls were discarded (phred score <20). The SSU Ref NR 99 database, (release 132) of SILVA [41] was used, which was preprocessed and indexed by the Kraken2 [42] with k-mer = 31. The final microbiome composition was estimated by Bracken [43].

2.10. Determination of small intestinal luminal pH

The content of the distal jejunum and ileum was collected, suspended in ultra-pure water at a ratio of 1:20, and its pH was measured with a 7310 inoLab pH benchtop meter (Xylem Analytics, Weilheim, Germany).

2.11. Histological analysis

Samples taken from the ileum were fixed in 10% formalin, embedded in paraffin, sectioned (5 μm), and stained with haematoxylin and eosin. Images were captured with Leica LMD6 microscope (Leica, Wetzlar, Germany) and epithelial damage, edema and cellular infiltration were assessed in a blinded fashion.

2.12. Immunohistochemistry

After routine FFPE specimen processing, deparaffinized sections underwent antigen retrieval (pH = 6 citrate buffer, at 95 °C for 15 min). After blocking endogenous peroxidase activity (3% H_2O_2 solution in PBS), the sections were blocked in appropriate sera (2.5% goat serum in PBS). Then, sections were incubated with primary anti-claudin 1 antibody (ab15098, 1:200, Abcam, Cambridge, UK) overnight in diluted blocking solution at 4 °C. After primary antibody incubations, the sections were washed three times in PBS and incubated for an hour with SignalStain® Boost IHC Detection Reagent (HRP, Rabbit, 8114, Cell Signaling Technology, Danvers, MA, USA). The secondary antibody was washed 3 times for 10 min and the specific signal was developed with diaminobenzidine (ImmPACT DAB EqV Peroxidase/HRP/Substrate, Vector Laboratories, Burlingame, CA, USA). The specific staining was visualized and images were acquired using a Leica LMD6 microscope (Leica, Wetzlar, Germany).

2.13. Data analysis

Statistical analysis of the data was performed with Kruskal Wallis test (in case of nonparametric values), or with one-way ANOVA, followed by Holm-Sidak post hoc test. Two-way repeated measures ANOVA was employed to compare the time course of weight losses. Outliers detected by Grubb's test were excluded from the analyses. A probability of $p < 0.05$ was considered statistically significant.

Alpha diversities were quantified by using the Shannon index (quantifying entropy of the distribution of taxa proportions). Taxa having at least support of 50 reads were considered as positive, others were discarded from the downstream analysis. The beta-diversities of the microbiome were assessed by applying Bray-Curtis distance measure (heat maps) and principal component analysis (PCA) was used for visualizing the microbiome composition. The differential abundance tests were performed using ANCOM [44] with Holm-Bonferroni corrected alpha of 0.05 as the rejection threshold. Zero abundance of taxa was replaced by a pseudocount 1.

To test statistical dependence between measured parameters Spearman's rank correlation coefficient (Rho-value) and the corresponding p-value were calculated for each possible pairing of inflammatory markers, absolute and relative bile acid concentrations and bacterial genus and family abundances at each sampling point across all animals. Resulting matrices of Rho-values were visualized as heat maps, where rows and columns were ordered according to complete linkage clustering based on Euclidean distances between the row and column vectors and ordering of the resulting dendrograms based on row and column means. Rows and columns not containing any non-zero Rho-values were omitted from heat maps. To control type I error arising from multiple comparisons individual p-values were corrected by the false discovery rate method (FDR; q-value according to Benjamini and Hochberg [45]). Significant associations were identified when $q < 0.05$. Correlation analysis, correction for multiple testing and heat map generation were performed using the R software bundle (version 3.4.4) [46].

3. Results

3.1. Indomethacin induces small intestinal injury, inflammation and pH alteration by a time-dependent manner

A single high dose (20 mg/kg per os) of indomethacin caused severe enteropathy in all rats, characterized by weight loss and different macroscopic signs of bowel injury, including ulcers, diaphragm-like strictures, ascites (three measures covered by the lesion score) and shortening of the small intestine. Despite the severe injury only one animal died during the experiment, 48 h after the administration of indomethacin. As Fig. 1A and B show, the severity of all macroscopic parameters increased gradually with time, being the most pronounced at 72 h. This was also confirmed by histological analysis, revealing an increasing number and severity of indomethacin-induced ulcerations with time (Fig. 1C). In parallel, the pH of the luminal content decreased progressively, but the change was moderate and reached significance only at 72 h (Fig. 1D).

In order to assess the severity of inflammatory reaction, we measured the amount of different inflammatory mediators and cytokines, which are known to participate in NSAID-enteropathy [25,47]. The tissue

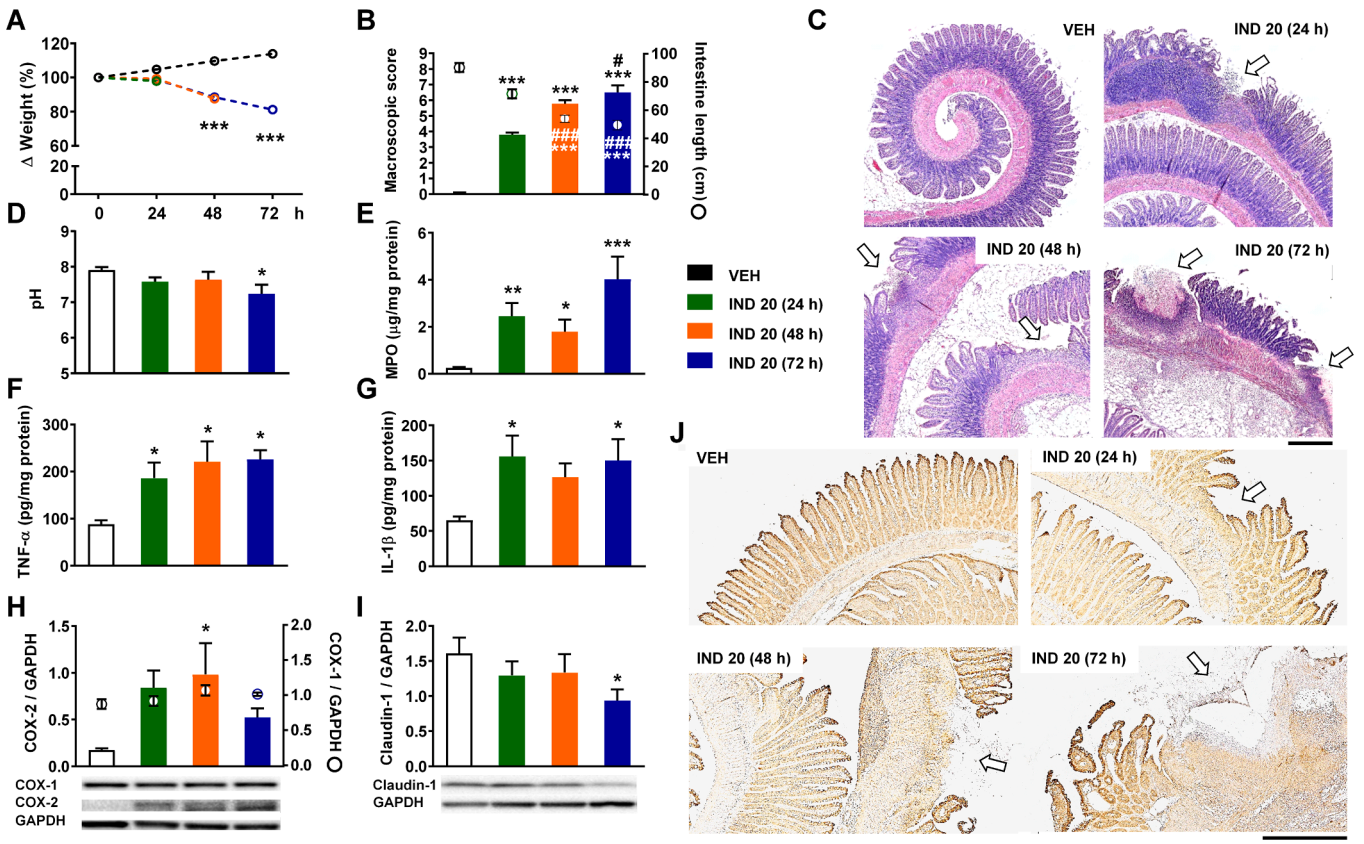

Fig. 1. Indomethacin induces inflammation and tissue damage in the small intestine. Indomethacin (IND, 20 mg/kg per os) after 24, 48 and 72 h changes animal weight, small intestinal length, luminal pH, and expression of inflammatory mediators, cytokines and claudin-1. Panel A: results are expressed as the mean ± SEM. Circles and bars indicate the mean + SEM. Panel C: representative histological images (scale bar: 500 μM, haematoxylin and eosin staining). Arrows denote indomethacin-induced ulcers, characterized by epithelial loss and inflammatory infiltration. Panel J: immunohistochemistry for claudin-1, arrows denote the loss of claudin-1 at the site of ulcerations (scale bar: 500 μM). For statistical analysis two-way repeated measures ANOVA followed by Holm-Sidak post hoc test (weight loss), Kruskal-Wallis test (macroscopic score), and one-way ANOVA with Holm-Sidak post hoc test (all other measurements) were used, n = 5–10/group. *p < 0.05, **p < 0.01, ***p < 0.001 compared to vehicle (VEH)-treated group; #p < 0.05, ###p < 0.001 compared to, "IND 20 (24 h)" group.

levels of MPO (a marker of neutrophil activation) and the pro-inflammatory cytokines TNF-α and IL-1β increased significantly in response to indomethacin treatment and were comparable at all time points (Fig. 1E–G). By contrast, the anti-inflammatory cytokine IL-10, which is produced by various cells to regulate the immune response, remained unchanged in all indomethacin-treated groups (54 ± 12, 49 ± 17, 49 ± 21 and 45 ± 18 pg/mg protein in vehicle- and indomethacin-treated animals after 24, 48 and 72 h, respectively, n = 9–10/group). Although the main pharmacological action of NSAIDs, including indomethacin, is the inhibition of COX enzymes, increased COX-2 expression is a representative marker of NSAID enteropathy [48]. COX-2 expression showed upregulation at all time points, being the highest and significant compared to control group at 48 h, whereas the level of the constitutive COX-1 was not affected by indomethacin (Fig. 1H). Finally, loss of tight junctions with increased intestinal permeability is also a hallmark of NSAID-enteropathy [48], therefore we measured the expression of claudin-1 by Western blot, which showed a gradual decline following indomethacin-treatment (Fig. 1I). The loss of claudin-1 was also confirmed by immunohistochemistry (Fig. 1J). Collectively, these data indicate that the level of pro-inflammatory mediators peaked already at 24 or 48 h after the administration of indomethacin, whereas the gradual decrease in claudin-1 expression was rather associated with the development of macroscopic and microscopic injury.

3.2. Indomethacin induces time-dependent bile dysmetabolism in the small intestine

Next, we determined the luminal concentration of 20 different bile acids (Table 1) in the distal small intestine by LC-MS/MS. The major bile acids in the control group were the primary bile acids cholic acid (CA), muricholic acid-α (MCA-α), MCA-β and their taurine conjugates, and the secondary bile acid hyodeoxycholic acid (HDCA) (Fig. 2). 24 h after the administration of indomethacin the luminal concentration of all bile acids, except lithocholic acid (LCA), decreased, though not all of them reached statistical significance. After 48 h, the concentration of most unconjugated bile acids decreased further (except HDCA and MCA-ω, which returned to the level of the control group), whereas the amount of most taurine and glycine conjugates started to rise. The same trends were evident after 72 h, when the level of most conjugated bile acids reached, or even exceeded that of the control levels, whereas the concentration of most unconjugated bile acids further decreased or remained at low levels (except HDCA, which showed further elevation).

Hence, indomethacin caused overt and time-dependent changes in the concentration of most bile acids, resulting in a markedly different bile acid profile. This was also confirmed by principal component analysis (PCA) of the data, which showed distinct clustering of samples in the vehicle- and indomethacin-treated groups, and also indicated a larger degree of variation within the control group (Fig. 3).

Calculating the percentage of each bile acid in the total small intestinal bile acid pool revealed that the proportions of taurine conjugates tended to increase already 24 h following indomethacin-treatment,

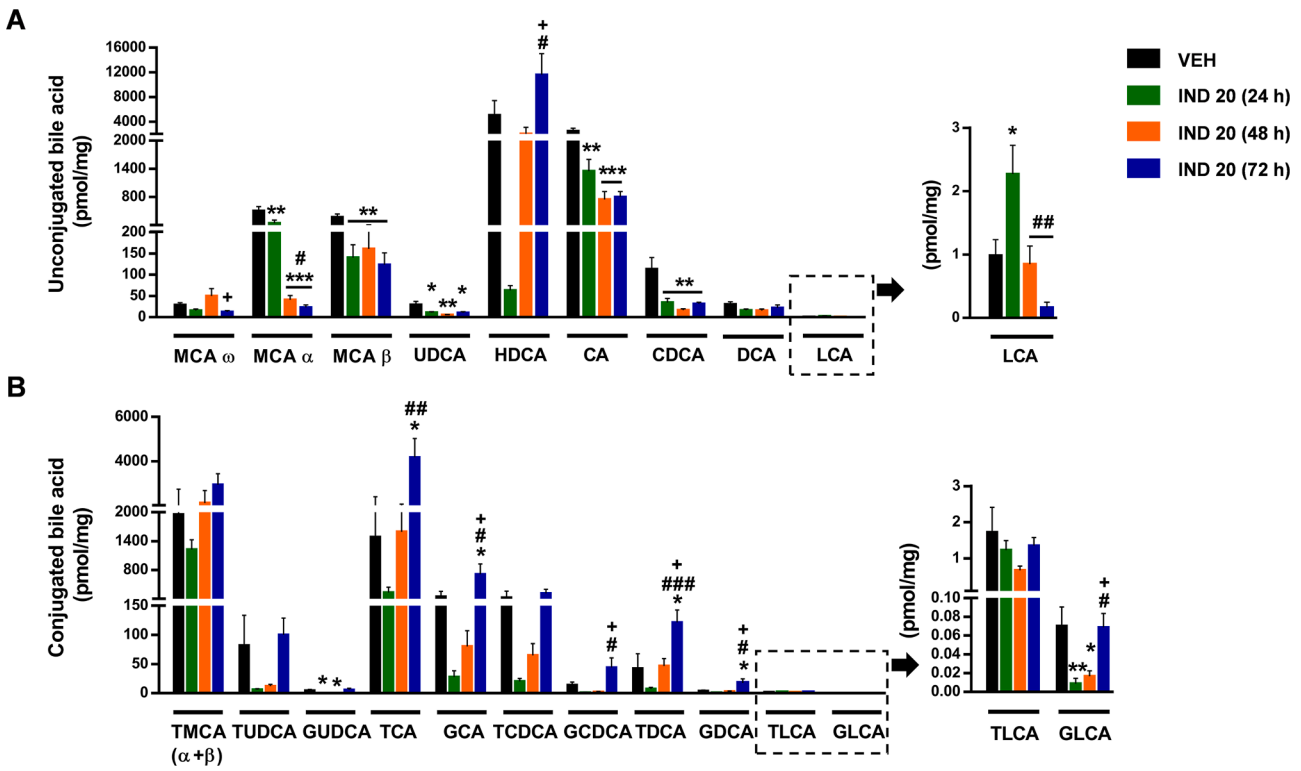

Fig. 2. The effect of indomethacin (IND, 20 mg/kg per os) after 24, 48 and 72 h on the small intestinal concentration of (A) unconjugated and (B) conjugated bile acids. Bile acids are ordered by increasing hydrophobicity. Bars indicate the mean + SEM. For statistical analysis one-way ANOVA with Holm-Sidak post hoc test was used, n = 9–10/group. *p < 0.05, **p < 0.01, ***p < 0.001 compared to vehicle (VEH)-treated group; #p < 0.05, ##p < 0.01, ###p < 0.001 compared to, "IND 20 (24 h)" group; +p < 0.05 compared to, "IND 20 (48 h)" group. MCA, muricholic acid; UDCA, ursodeoxycholic acid; HDCA, hyodeoxycholic acid; CA, cholic acid; CDCA, chenodeoxycholic acid; DCA, deoxycholic acid; LCA, lithocholic acid; T, respective taurine conjugates; G, respective glycine conjugates.

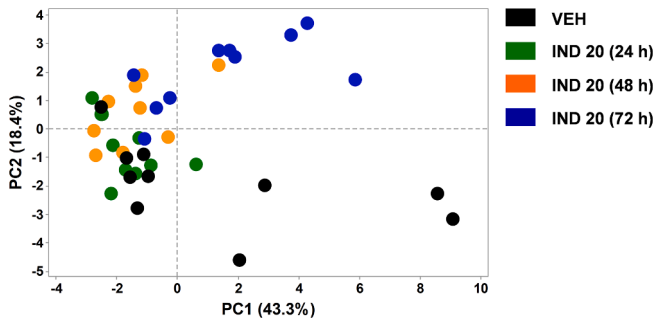

Fig. 3. Principal component analysis (PCA) score plot comparing the small intestinal bile acid composition of rats treated with either vehicle (VEH) or indomethacin (IND). Indomethacin-treated animals were sacrificed at 24, 48 or 72 h following treatment. The percentage of variation explained by the principal components (PC1 and PC2) is indicated on the axes.

despite the temporary reduction in their absolute concentrations (Fig. 4). Of note, the proportion of the hydrophilic TMCA(α + β), the most abundant taurine conjugate, showed significant 2.4-fold elevation, making up almost 40% of the total ileal bile acid pool at this time point. By contrast, at 24 h the proportions of all glycine conjugates showed an opposite trend towards reduction, in parallel with the reduction of their absolute concentrations. After 48 and 72 h, however, there was no major difference between the proportional changes of taurine and glycine conjugates, as both increased gradually with time. The only exceptions are TMCA(α + β) and TLCA, which both decreased after their initial rise to match the control group at 72 and 48 h, respectively. The proportional changes of unconjugated bile acids reflected mainly the changes in their absolute values, and in most cases showed time-dependent reductions (with the most notable exception of HDCA). However, the percentage of the hydrophobic deoxycholic acid (DCA) tended to increase first, in contrast to the reduction of its absolute concentration.

Altogether, these data indicate that the most prominent alterations of the small intestinal bile acid metabolome were an initial temporary reduction in the concentration of almost all bile acids, and a gradual, time-dependent elevation of most conjugated bile acids, in parallel with the reduction of the unconjugated ones. These changes were also reflected by the amount of total ileal bile acids (which tended to decrease first (p = 0.07), then increased gradually, being the highest at 72 h), and by the ratio of conjugated to total bile acids, which was significantly increased at all three time points (Fig. 5A, B). In addition, because the proportion of taurine-conjugated bile acids increased already after 24 h, whereas that of the glycine conjugates tended to decrease first, the ratio of glycine to taurine-conjugated bile acids was decreased in all indomethacin-treated groups (Fig. 5C).

Based on the biliary effects of indomethacin [10], we expected a significant elevation of the secondary bile acids in the ileum, but indomethacin treatment showed no characteristic effect on either their concentrations or percentage values, and their changes over time showed different patterns (Figs. 2 and 4). When the ratio of secondary to total bile acids was calculated, it showed a temporary reduction, followed by a significant elevation (Fig. 5D), but this mainly reflected the changes of the relatively hydrophilic HDCA, the major secondary bile acid in the small intestine. Similarly, in contrast to our original expectations, the mean hydrophobicity index of the small intestinal content decreased 24 and 48 h after indomethacin treatment, then returned back to the level of control group (Fig. 5E), which changes were mainly determined by the large proportion of the hydrophilic TMCA(α + β).

Finally, the changes in the amount of total ileal bile acids prompted us to measure the expression of some key players in bile acid transport and synthesis [49]. In the ileum, most bile acids are reabsorbed by the

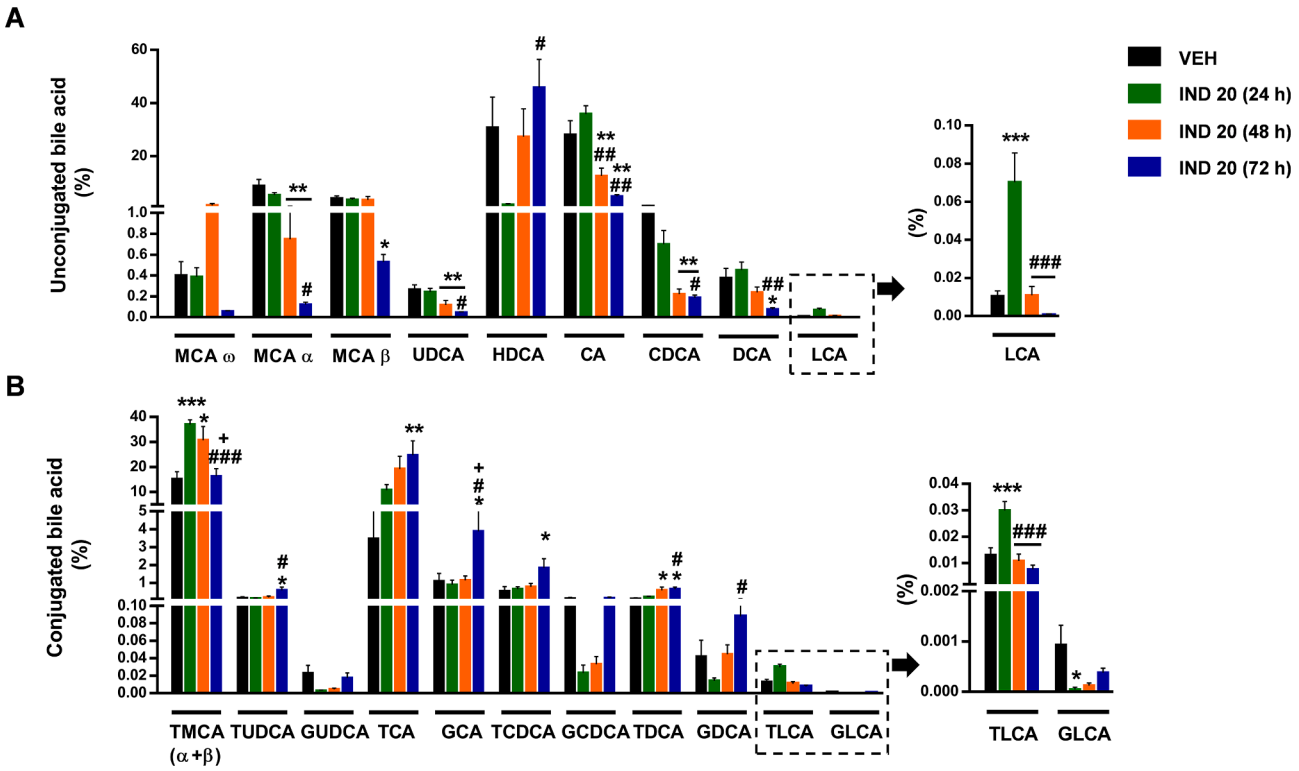

Fig. 4. The effect of indomethacin (IND, 20 mg/kg per os) after 24, 48 and 72 h on the small intestinal proportion of (A) unconjugated and (B) conjugated bile acids. Bile acids are ordered by increasing hydrophobicity. Bars indicate the mean + SEM. For statistical analysis one-way ANOVA with Holm-Sidak post hoc test was used, n = 9–10/group. *p < 0.05, **p < 0.01, ***p < 0.001 compared to vehicle (VEH)-treated group; #p < 0.05, ##p < 0.01, ###p < 0.001 compared to, "IND 20 (24 h)" group; +p < 0.05 compared to, "IND 20 (48 h)" group. MCA, muricholic acid; UDCA, ursodeoxycholic acid; HDCA, hyodeoxycholic acid; CA, cholic acid; CDCA, chenodeoxycholic acid; DCA, deoxycholic acid; LCA, lithocholic acid; T, respective taurine conjugates; G, respective glycine conjugates.

apical sodium-dependent bile acid transporter (ASBT), then bind to the nuclear farnesoid X receptor (FXR), which thereafter inhibits the hepatic synthesis of bile acids via a negative feedback. As Fig. 5F and G show, the intestinal expression of both *Fxr* and *Asbt* mRNA decreased after 48 h and 72 h, respectively, suggesting that an impaired bile acid uptake and dysregulation of FXR-signaling may contribute to the elevated intestinal bile acid level measured at 72 h. On the other hand, the initial reduction in total bile acid concentration at 24 h may be due to the dramatic temporary reduction in the hepatic expression of *Cyp7a1*, the first and rate-determining enzyme of bile acid synthesis (Fig. 5H).

3.3. Indomethacin induces time-dependent small intestinal dysbiosis

The microbiota of vehicle- and indomethacin-treated animals was determined by deep sequencing of 16S rRNA. In the distal small intestine of control rats, the vast majority (89.8%) of identified taxa belonged to the Firmicutes phylum (with the most abundant genera being *Lactobacillus*, *Romboutsia*, *Turicibacter* and *Clostridium sensu stricto 1*), followed by Bacteroidetes and Proteobacteria (8.0 and 1.3%, respectively). Indomethacin caused significant changes in the proportion of several bacteria (Fig. 6), resulting in a markedly different overall microbiota profile compared to that of control rats, as shown by the PCA score plot (Fig. 6C). In general, these changes were characterized by reduction in the relative abundance of Gram-positive genera, accompanied by the expansion of Gram-negative ones (Fig. 6A, B), in agreement with previous reports [8,20,50].

Analysing the qualitative presence of bacteria in the luminal content (Fig. 7) also revealed the disappearance of several Gram-positive genera after indomethacin treatment, including *Christensenellaceae R-7 group*, *Clostridioides*, *Paenibacillus*, *Paraclostridium*, *Pediococcus* and *Terrisporobacter* (all belonging to Firmicutes), and the appearance of Gram-negative taxa, such as *Luteibacter*, *Morganella*, *Sodalis*, *Shimwellia*, *Vibrio* (Proteobacteria) or *Akkermansia* (Verrucomicrobia). On the other hand, the proportions of *Dubosiella* and *Bifidobacterium*, despite being Gram-positive bacteria, tended to increase in response to indomethacin treatment (Fig. 6A).

There were also some notable differences between the temporal changes of some taxa. Namely, genera belonging to the Gammaproteobacteria (*Pantoea*, *Serratia*, *Escherichia-Shigella*, *Enterobacter* and *Rodentibacter*) and *Parasutterella* (a member of Betaproteobacteria) tended to decrease after peaking at 24–48 h, in parallel with the appearance and expansion of Gram-negatives belonging to other bacterial classes, such as *Bilophila* (Deltaproteobacteria), *Bacteroides* (Bacteroidia) and *Fusobacterium* (Fusobacteriia) (Fig. 6B).

The Shannon indices of vehicle- and indomethacin-treated groups showed only minor differences, suggesting that despite the marked changes in microbiota composition indomethacin had no major effect on microbial diversity (Fig. 6D).

We also aimed to assess whether indomethacin has any direct effect on the growth of bacteria, which could potentially contribute to the observed small intestinal dysbiosis. As Table 2. shows, indomethacin (up to 256 mg/L) had no significant effect on the growth of tested Gram-positive and Gram-negative strains in the broth microdilution assay.

3.4. Correlations between indomethacin-induced inflammation, bile dysmetabolism and dysbiosis

To synthetize the obtained data, Spearman's correlation analysis was performed to explore the associations between the measured injury markers, the absolute and relative concentration of bile acids, and the proportion of identified bacterial genera and families. Calculated Rho-values (n = 5305) were visualized as heat maps with dendrograms to indicate related variables.

Most unconjugated bile acids, irrespective of their primary or

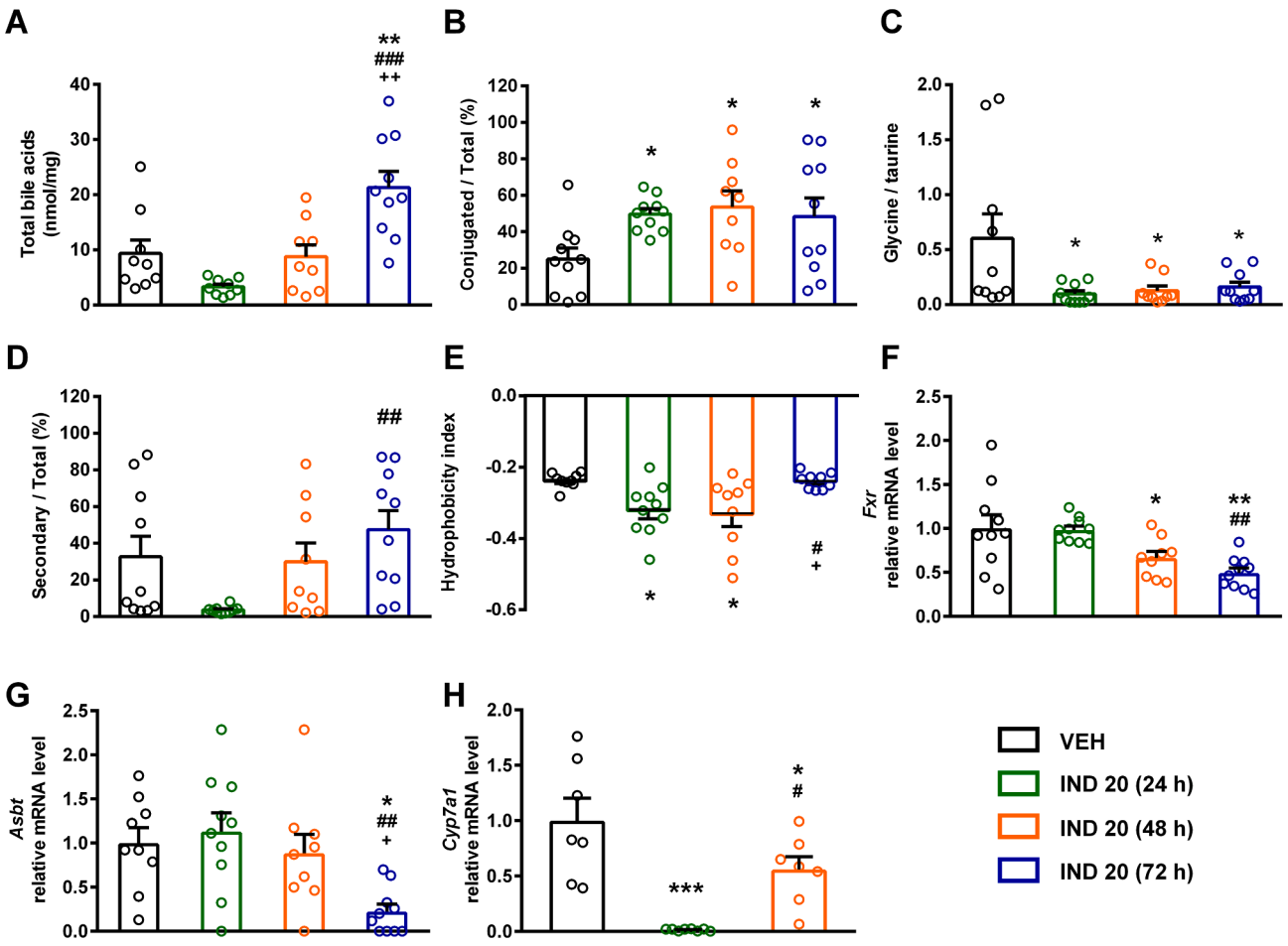

Fig. 5. Indomethacin alters the small intestinal bile acid metabolome. The effect of indomethacin (IND, 20 mg/kg per os) at different time points on (A) total ileal bile acid level, (B) the ratio of conjugated to total ileal bile acids, (C) the ratio of glycine to taurine conjugates, (D) the ratio of secondary to total ileal bile acids, (E) the mean hydrophobicity index, (F, G) ileal mRNA levels of FXR and ASBT and (H) hepatic mRNA level of CYP7A1. Circles represent the data of each rat, bars indicate the mean + SEM. For statistical analysis one-way ANOVA was used with Holm-Sidak post hoc test, n = 7–10/group. *p < 0.05, **p < 0.01 compared to vehicle (VEH)-treated group; #p < 0.05, ##p < 0.01, ###p < 0.001 compared to, "IND 20 (24 h)" group; +p < 0.05, ++p < 0.01 compared to, "IND 20 (48 h)" group.

secondary nature, clustered together and correlated negatively with the severity of injury (in particular CA and MCA-α with the lesion score), whereas the majority of taurine conjugates, together with HDCA, grouped into another cluster and tended to correlate positively with injury and inflammation (Fig. 8). These results reflect most likely the similarity in temporal changes of conjugated bile acids and inflammatory markers, rather than indicating the contribution of these bile acids to inflammation. They also suggest that changes in the concentration or proportion of particular hydrophilic or hydrophobic bile acids are not major determinants of the severity of damage.

Calculating the correlations between bacterial abundances and tissue injury markers revealed distinct clustering of the genera *Bacillus*, *Romboutsia*, *Lactobacillus*, *Candidatus Arthromitus*, *Streptococcus*, *Ruminococcaceae UCG-014* and *Turicibacter*, all belonging to Firmicutes, which correlated negatively with the severity of damage (Fig. 9A). By contrast, the genus *Bacteroides* tended to correlate positively with inflammation and negatively with the expression of claudin-1, and clustered together with *Parasutterella*, *Morganella* (Proteobacteria) and *Dubosiella* (Firmicutes). Several genera of the Gammaproteobacteria, on the other hand, formed a third cluster together with *Bifidobacterium* and *Clostridium sensu stricto 1*, showing rather negative correlation with injury markers (in particular with the lesion score and MPO level). Similar associations were found at the family level (Fig. 9B), in which most families showing inverse correlation with tissue injury belonged to the Firmicutes, whereas families showing rather positive correlation with mucosal damage and inflammation belonged to either the Bacteroidetes (*Muribaculaceae*, *Prevotellaceae*, *Bacteroidaceae*) or Proteobacteria (*Pasteurellaceae*, *Enterobacteriaceae*, *Burkholderiaceae*).

The present analysis also revealed numerous positive and negative associations between the abundances of some bacteria and percentage or absolute concentrations of distinct bile acids (Figs. 10 and 11), although when individual p-values were corrected for multiple testing, only some of them remained significant. The strongest positive correlations were found between some Firmicutes (*Lactobacillaceae*, *Ruminococcaceae*, *Peptostreptococcaceae*, *Clostridiaceae 1*, *Lachnospiraceae*) and the proportion and concentration of the unconjugated bile acids chenodeoxycholic acid (CDCA) and MCA(α). This resonates well with the findings that deconjugation of bile acids is mainly performed by Firmicutes, like *Clostridium*, *Enterococcus*, *Ruminococcus* and *Lactobacillus* [14,52]. In addition, several taxa of the Gammaproteobacteria tended to correlate positively with the percentage of unconjugated bile acids (in particular, *Escherichia-Shigella* with LCA) and some taurine conjugates (TMCA(α + β), TLCA), and negatively with the concentrations of most conjugates, HDCA and total bile acids.

4. Discussion

The present study was designed to explore the alterations in small

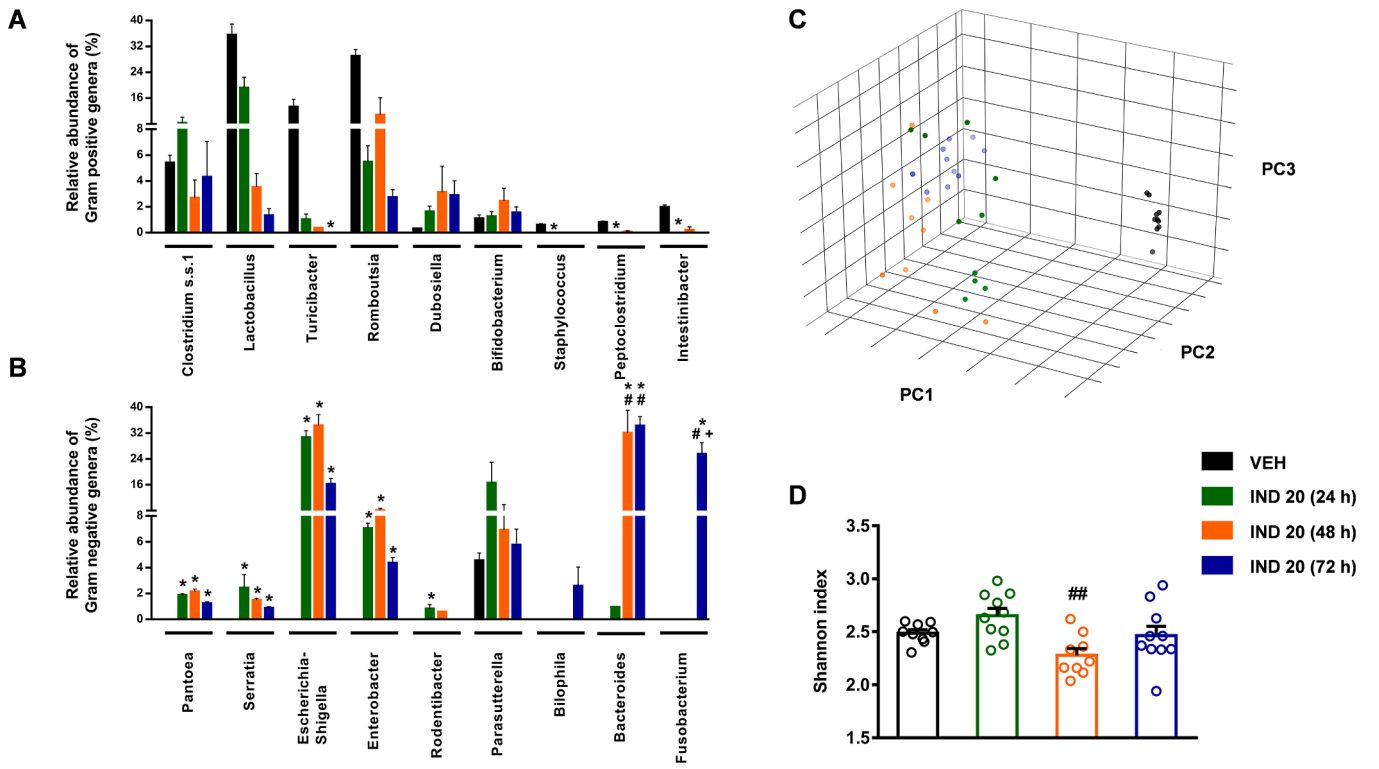

Fig. 6. The effect of indomethacin (IND, 20 mg/kg per os) after 24, 48 and 72 h on the small intestinal proportion of the most abundant (A) Gram-positive and (B) Gram-negative bacteria. Bars indicate the mean + SEM. The differential abundance tests were performed using ANCOM with Holm-Bonferroni correction for multiple comparison, n = 9–10/group. *p < 0.05 compared to vehicle (VEH)-treated group; #p < 0.05 compared to, "IND 20 (24 h)" group; +p < 0.05 compared to, "IND 20 (48 h)" group. Panel C: Principal component analysis (PCA) score plot comparing the small intestinal microbiota composition of rats treated with either vehicle (VEH) or indomethacin (IND). Indomethacin-treated animals were sacrificed at 24, 48 or 72 h following treatment. Panel D: The effect of indomethacin on small intestinal bacterial diversity, estimated by the Shannon index. Circles represent the data of each rat, bars indicate the mean ± SEM. For statistical analysis one-way ANOVA was used with Holm-Sidak post hoc test, n = 9–10/group. ##p < 0.01 compared to, "IND 20 (24 h)" group.

intestinal bile acid composition in a widely used animal model of NSAID-enteropathy. Considering that bile acids and intestinal bacteria are closely interrelated, we also determined the time-dependent changes of the ileal microbiota, and aimed to identify associations between bile acids, bacteria and tissue injury.

There are several evidence that NSAIDs increase the cytotoxicity of bile, which likely plays an important role in the pathogenesis of enteropathy [6–9]. However, little is known about the effects of NSAIDs on the intestinal bile acid composition, and whether changes in particular bile acids correlate with the development of mucosal damage and dysbiosis. Therefore, in the present study we assessed the mucosal injury and inflammation in the distal small intestine following indomethacin administration, and also measured the luminal concentration of bile acids and composition of microbiota at the same site. Moreover, in order to better understand the dynamics of their changes, we measured them at 3 different time points.

The finding that a single, high dose of indomethacin induces severe enteropathy within 24 h is in agreement with literature data [21,53]. We also found that the mucosal inflammatory reaction peaked at 24–48 h, whereas the weight loss of animals, visually visible signs of enteropathy (ascites, adhesions, ulcers, bowel shortening), histological damage and loss of intestinal barrier (claudin-1 expression) showed continuous progression with time.

Our results revealed marked, time-dependent alterations of ileal bile acids in response to indomethacin, which in general could be divided into 2 phases. At the first time point measured, the luminal concentration of almost all individual bile acids decreased, in parallel with the development of mucosal injury and inflammation. Although a detailed analysis of the transporters and enzymes involved in bile acid metabolism was beyond the scope of this study, we measured the expression of some key factors, including CYP7A1. This hepatic enzyme initiates the classic bile acid biosynthetic pathway [49], and is known to be repressed by inflammatory cytokines and indomethacin [54]. In agreement with this, we also found a dramatic temporary reduction in the expression of *Cyp7a1*, which likely accounted for the initial decline of ileal bile acid pool.

At the same time, the relative amount of taurine conjugates started to rise, resulting in an increased ratio of conjugated to total bile acids. Because deconjugation of bile acids is carried out by bile salt hydrolases (BSHs), enzymes expressed mainly by Gram-positive bacteria [14], the marked increase in the ratio of conjugated to total bile acids is most likely due to the gradual loss of Gram-positive strains, which was evident already 24 h after indomethacin. Indeed, we found strong positive correlation between some bacterial families possessing deconjugating activity, such as *Lactobacillaceae*, *Ruminococcaceae* and *Clostridiaceae 1* [14], and the absolute and relative concentration of unconjungated bile acids. Although we found positive associations between the Gammaproteobacteria and unconjugated bile acids as well, these taxa also correlated with some taurine conjugates and with the proportion of all conjugates, suggesting that these associations lack causality and reflect only the peculiar temporal changes of these bacteria, as discussed below.

The proportion of glycine conjugates, in contrast to the taurine forms, decreased first, resulting in a reduced glycine to taurine ratio. This ratio remained low at later time points as well, as the levels of glycine conjugates, despite their rise in the later phase, could not catch up with those of the taurine ones. Although the reason of this shift towards taurine conjugated bile acids remains to be established, it may be due at least partly to the indomethacin-induced dysbiosis as well. For example, in a recent *in vitro* correlation analysis, a delay in taurine

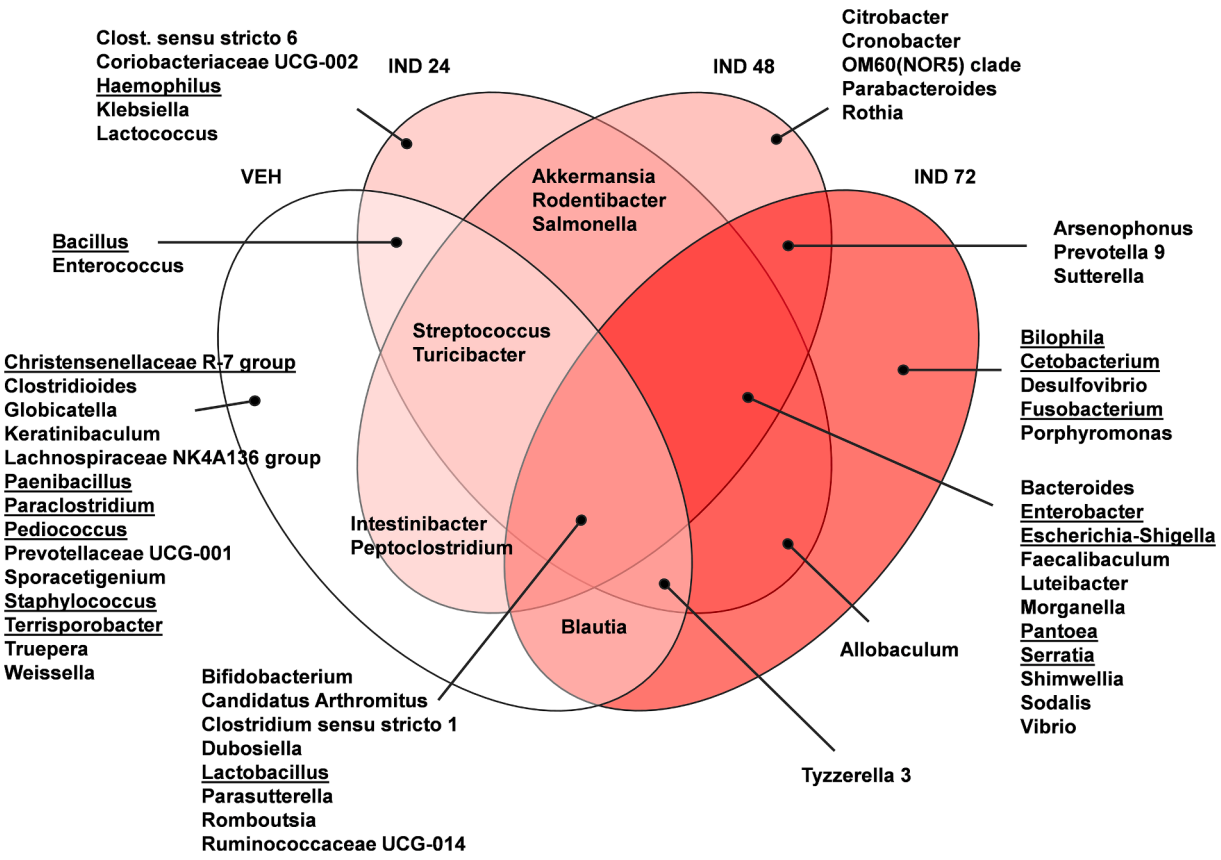

Fig. 7. Venn diagram of the genera present in the small intestinal content of rats treated with either vehicle (VEH) or indomethacin (IND). Indomethacin-treated animals were sacrificed at 24, 48 or 72 h following treatment. Underlined genera are present in at least half of the animals of each group.

cleavage was associated with a lower abundance of *Ruminococcus*, and with a greater abundance of *Parasutterella* and *Akkermansia* [52], which bacterial changes occured already 24 h following the gavage of indomethacin in our study.

The later phase of indomethacin-evoked bile acid alterations, observed after 48 and 72 h, was characterized by a gradual, time-dependent elevation of most conjugated, as well as total amount of bile acids, and the reduction of most unconjugated ones, with the exception of HDCA. These changes were most likely driven mainly by two factors occuring at the same time, namely, the increased synthesis of bile acids and the continuous decline of Gram-positive bacteria and their deconjugation capacity. The first may arise from the disturbed FXR-signaling, which decreased gradually after 48 h, and would otherwise control the activity of CYP7A1 and bile acid synthesis via a negative feedback mechanism [55]. As our results show, indomethacin also repressed the expression of ASBT, the ileal transporter responsible for the reuptake of bile acids. This is in agreement with previous studies [56], and may contribute to both impaired activation of the nuclear FXR, and increased luminal proportion of conjugated bile acids, for which it has higher affinity than for the unconjugated forms [57].

Another important finding of the present study is that indomethacin did not increase the hydrophobicity index of bile in the ileum, in contrast to the biliary tract [10,11]. Although the hydrophobic secondary bile acids LCA, TDCA and GDCA showed slight elevations at different time points, this has probably limited relevance, considering their low amounts, and the simultaneous elevation and much higher levels of TMCA(α + β), one of the most hydrophilic bile acids [34]. Accordingly, indomethacin decreased instead of increasing the mean hydrophobicity index of small intestinal bile at 24 and 48 h, which returned to the normal level at 72 h, and was mainly determined by the large proportion of TMCA(α + β). At present we cannot explain why indomethacin decreased the proportion of TMCA(α) and TMCA(β) in the bile [10] and increased it in the ileum. However, it is of note that Lu et al. [18] reported similar changes in the hepatic and ileal concentration of TMCA in ibuprofen-treated mice. Hence, the effect of NSAIDs on small intestinal bile acid composition is likely different from that reported in the biliary tract, and changes in the percentage of secondary bile acids and hydrophobicity index do not appear to be important in the development of NSAID-enteropathy. It should be noted that our results do not argue against the concept that NSAIDs including indomethacin increase bile citotoxicity [6–9], only suggest that other mechanisms than changes in the proportion of secondary bile acids result in it (like, for example, NSAID-induced alterations in micellar toxicity [6,7,9]). It is also supported by our correlation analysis, in which the direction of associations between bile acids and injury markers depended mainly on the state of conjugation of bile acids, and not on their hydrophobicity. Although these correlations reflect most likely the temporal changes of individual bile acids, at present, we cannot fully exclude the possibility that they also indicate some causal relationship. For example, the positive correlation between taurine conjugates and mucosal injury could be partly explained by the increased availability of organic sulfur and expansion of colitogenic sulfate-reducing bacteria, like *Bilophila* and *Desulfovibrio* [58,59], which both appeared 72 h after the administration of indomethacin.

The changes we observed in small intestinal microbiota in response to indomethacin correspond well to those reported previously in rodents treated with different NSAIDs [8,20,21,23,50]. The enrichment of Gram-negative bacteria is believed to contribute to NSAID-enteropathy [25], but also the decrease in Gram-positive bacteria may be damaging, because several taxa, including members of *Lactobacillaceae* [21], *Clostridia* [60] and *Actinobacteria* [61], exert anti-inflammatory and mucosal protective effects. Indeed, in the present study the severity of mucosal

Table 2
The minimum inhibitory concentration (MIC) of indomethacin against various Gram-positive and Gram-negative bacteria.

Bacterium	Description	MIC mg/L		
		Indo-methacin	Vanco-mycin	Cipro-floxacin
Staphylococcus aureus ATCC 29213	Methicillin-sensitive strain (MSSA)	>256	1	≤0,5
Staphylococcus aureus ATCC 33591	Methicillin-resistant strain (MRSA)	>256	1	≤0,5
Enterococcus faecalis ATCC 51299	*vanB* vancomycin-resistant strain	>256	64	2
Enterococcus faecalis ATCC 29212	Vancomycin-sensitive strain	>256	2	1
Bacterium	Description	MIC mg/L Indo-methacin	Imipenem	Colistin
Acinetobacter baumannii ATCC BAA1605	MDR strain isolated from the sputum of a Canadian soldier	>256	16	<0,5
Klebsiella pneumoniae ST258 clone K 160/09 [51]	Clinical isolate with Carbapenemase (KPC), resistant to carbapenem and colistin	>256	>256	64
Escherichia coli ATCC 25218	Quality control strain for susceptibility testing of beta-lactam antibiotics, TEM-1 β-lactamase-producing strain	>256	1	4
Pseudomonas aeruginosa ATCC 27853	Quality control strain for E-test Metallo beta-lactamase strip	>256	1	2

inflammation correlated mainly with the abundance of Gram-negative genera (*Bacteroides*, *Parasutterella*, *Morganella*), whereas negative associations were found between inflammation and many Gram-positive bacteria.

Our analysis, however, also revealed that changes in distinct Gram-negative bacteria followed different patterns. Gammaproteobacteria increased rapidly, but started to decline after 48 h and were partially replaced by *Bilophila*, *Bacteroides* and *Fusobacterium*, which increased only later. These findings may explain some apparent contradictions between earlier studies, in which the composition of microbiota was assessed at different single time points, and for example, showed either no change [21] or an increase in *Bacteroides* after indomethacin treatment [22]. The late decrease in Gammaproteobacteria also explains the lack of clear positive correlation between these bacteria and tissue injury markers, despite the large body of evidence suggesting their role in the development of mucosal damage [8,49,62]. Furthermore, it may also account for their apparent negative correlation with conjugated bile acids, despite the lack of evidence for BSH expression and deconjugation by these strains [14,63].

The exact causes of NSAID-induced dysbiosis are still poorly understood, but besides inflammation-related perturbations in the microenvironment [64] and alterations in bile acids [26], also changes in luminal pH [65,66] may contribute to it. In addition, some NSAIDs possess direct antibacterial effects as well [67]. Although we focused mainly on characterizing the time-dependent changes of bacteria after indomethacin treatment, and not on the underlying mechanisms, we performed an *in vitro* antibacterial activity assay, and the results argue against a direct effect of indomethacin on the growth of bacteria. We also measured the pH in the lumen of small intestine, which, on the other hand, showed a moderate, gradual, time-dependent decline. Nevertheless, it should be considered that acidic pH is less favourable to *Bacteroides* and more favourable to the growth of numerous strains belonging to Firmicutes [65]. Therefore, the observed changes in microbiota do not correspond to the reported pH tolerance of bacteria, suggesting that alterations in luminal pH do not have a major role in indomethacin-induced dysbiosis.

A potential limitation of our study is that we used a single, large dose of indomethacin to induce enteropathy. Although this is one of the most widely used animal models [19,21,25,29,30,50,53], it may not adequately represent the enteropathy caused by long-term NSAID use in humans. Nevertheless, the inflammation caused by a single dose of

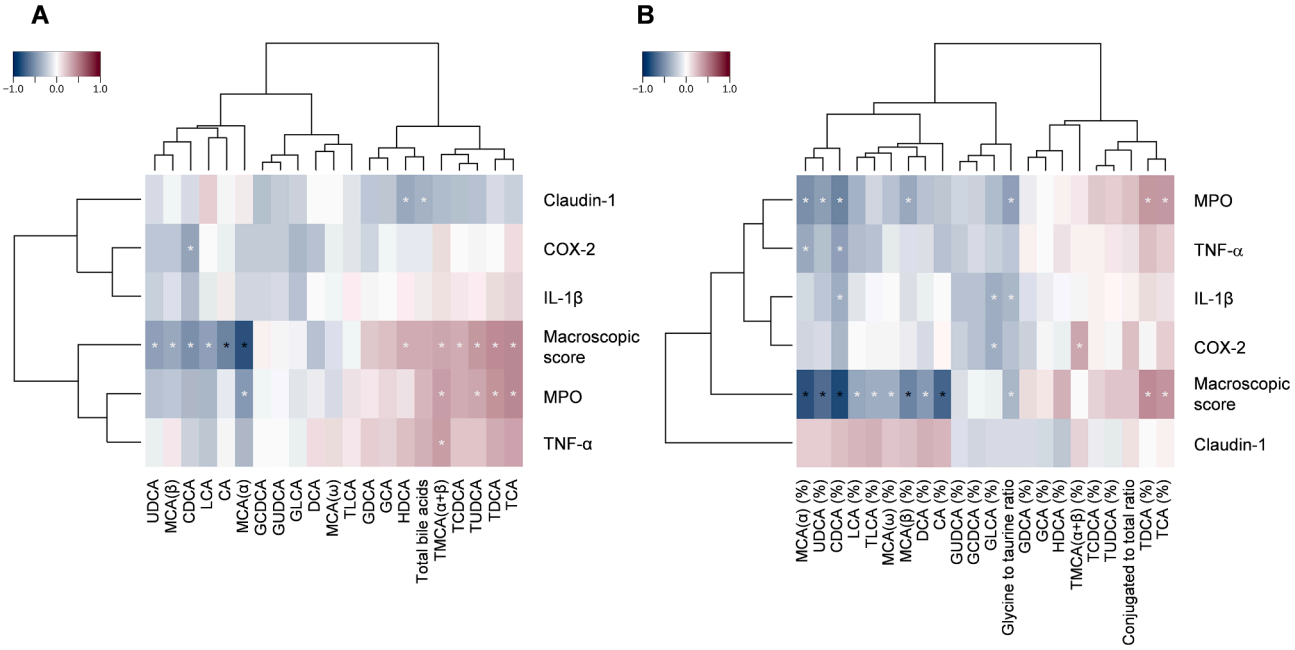

Fig. 8. Heat map of Spearman's correlation coefficients between tissue injury markers and (A) the small intestinal luminal concentration or (B) the proportion of individual bile acids. Individual p values were corrected by the false discovery rate method according to Benjamini and Hochberg. White asterisk: uncorrected $p < 0.05$, black asterisk: $q < 0.05$.

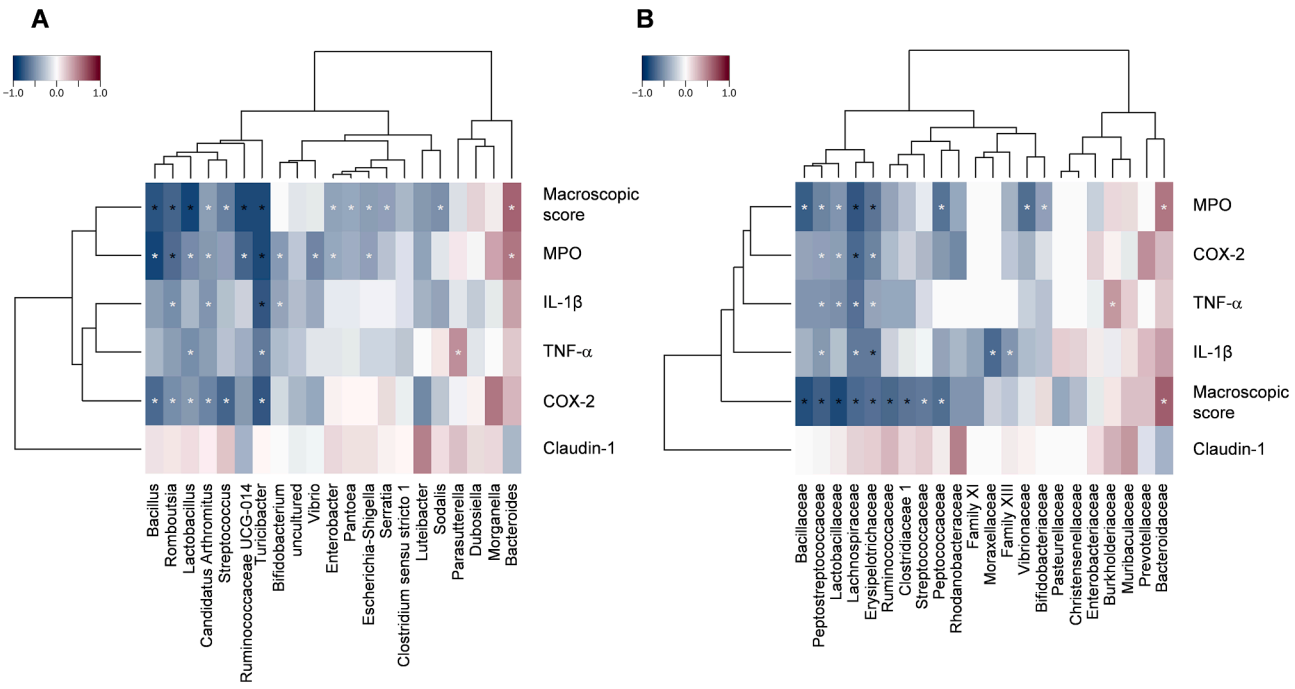

Fig. 9. Heat map of Spearman's correlation coefficients between tissue injury markers and the small intestinal relative abundance of (A) bacterial genera or (B) bacterial families. Individual p values were corrected by the false discovery rate method according to Benjamini and Hochberg. White asterisk: uncorrected $p < 0.05$, black asterisk: $q < 0.05$.

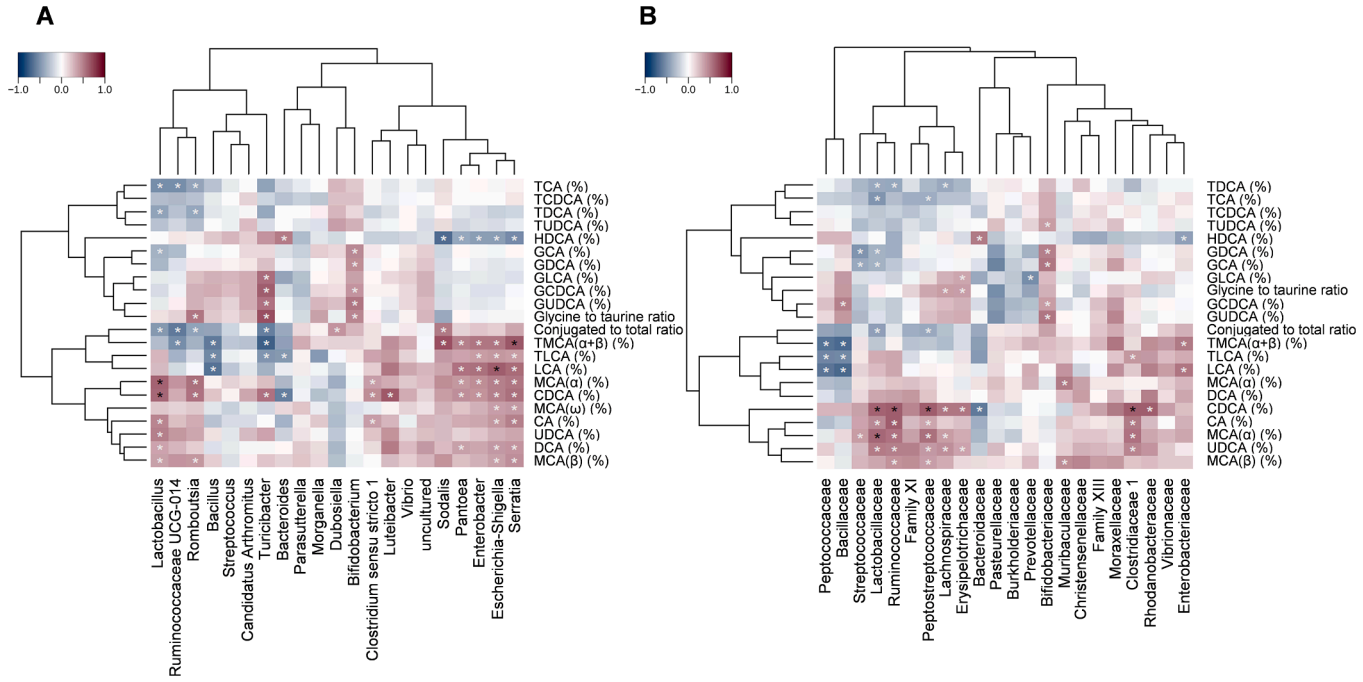

Fig. 10. Heat map of Spearman's correlation coefficients between the small intestinal luminal proportion of individual bile acids and the relative abundance of (A) bacterial genera or (B) bacterial families. Individual p values were corrected by the false discovery rate method according to Benjamini and Hochberg. White asterisk: uncorrected $p < 0.05$, black asterisk: $q < 0.05$.

indomethacin and chronic use of diclofenac [68] involves similar mediators in rats, including MPO, TNF-α and TLR4, and also the changes in microbiota are similar (i.e. expansion of Gram-negative bacteria and loss of Gram-positives). In addition, the enteropathy caused by indomethacin in rodents is similar in many aspects to that in humans, including the localization of ulcers, changes in intestinal permeability and responses to some treatments [5]. However, there are undoubtedly differences between animal models and humans, and our findings have to be confirmed in human studies as well.

In conclusion, here we characterized for the first time the time-dependent alterations of small intestinal bile acid composition following NSAID-treatment, and the associations between bile acids, bacteria and mucosal injury. We showed that indomethacin induced marked changes in ileal bile acid composition. These, however, were

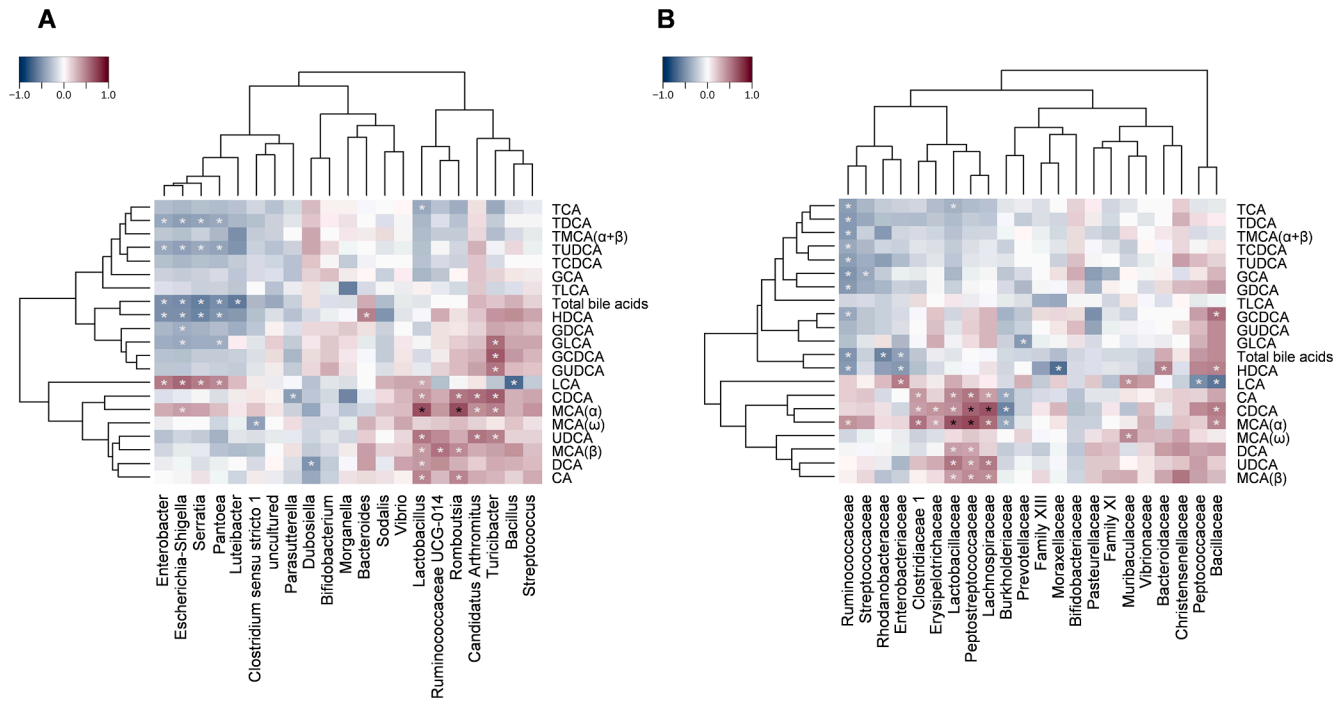

Fig. 11. Heat map of Spearman's correlation coefficients between the small intestinal luminal concentration of individual bile acids and the relative abundance of (A) bacterial genera or (B) bacterial families. Individual p values were corrected by the false discovery rate method according to Benjamini and Hochberg. White asterisk: uncorrected $p < 0.05$, black asterisk: $q < 0.05$.

mainly characterized by a shift towards a higher proportion of conjugated bile acids, and not by a significant elevation of hydrophobic secondary bile acids, which argues against the role of increased bile hydrophobicity in the pathogenesis of NSAID-enteropathy. The rise in conjugates occured in parallel with the loss of Gram-positive deconjugating bacteria, and correlated positively with mucosal damage. In general, Gram-negative bacteria increased with time and correlated positively with tissue damage, but we also identified notable differences in their temporal changes. Although the complex interactions of bile, bacteria and inflammation still remain insufficiently understood, our comprehensive time course and correlation analysis may help to decipher the complex pathogenesis of NSAID-enteropathy.

CRediT authorship contribution statement

Bernadette Lázár: Conceptualization, Formal analysis, Investigation, Writing - original draft. **Szilvia B. László:** Formal analysis, Investigation. **Barbara Hutka:** Formal analysis, Investigation. **András S. Tóth:** Formal analysis, Investigation. **Amir Mohammadzadeh:** Formal analysis, Investigation. **Eszter Berekméri:** Formal analysis, Investigation. **Bence Ágg:** Formal analysis, Investigation. **Mihály Balogh:** Formal analysis, Investigation. **Viktor Sajtos:** Formal analysis, Investigation. **Kornél Király:** Writing - review & editing. **Mahmoud Al-Khrasani:** Writing - review & editing, Funding acquisition. **Anna Földes:** Formal analysis, Investigation. **Gábor Varga:** Writing - review & editing. **Nóra Makra:** Formal analysis, Investigation. **Eszter Ostorházi:** Formal analysis, Investigation. **Dóra Szabó:** Writing - review & editing. **Balázs Ligeti:** Formal analysis, Investigation. **Ágnes Kemény:** Formal analysis, Investigation, Funding acquisition. **Zsuzsanna Helyes:** Writing - review & editing, Funding acquisition. **Péter Ferdinandy:** Writing - review & editing, Funding acquisition. **Klára Gyires:** Writing - review & editing. **Zoltán S. Zádori:** Conceptualization, Writing - original draft, Writing - review & editing, Funding acquisition, Supervision.

Declaration of Competing Interest

Péter Ferdinandy is the founder and CEO of Pharmahungary, a group of R&D companies. Bence Ágg was employed by Pharmahungary Group.

Acknowledgments

The authors wish to express their thanks to Veronika Pol-Maruzs, Judit Simon, Patrik Pálnok, Ádám Lakos and Dávid Szili for their technical assistance. The graphical abstract contains artworks produced by Servier Medical Art (http://smart.servier.com).

The research was supported by the National Research, Development and Innovation Office of Hungary (NKFI FK 124878), GINOP-2.3.2-15-2016-00048 and EFOP-3.6.2-16-2017-00006, by the Scientific and Innovative Research Fund of Semmelweis University (SE STIA-KF-17), and by the Higher Education Institutional Excellence Programme of the Ministry of Human Capacities, within the framework of the Neurology and the Therapy thematic programmes of the Semmelweis University (FIKP 2018), and by the Research Excellence Programme of the National Research, Development and Innovation Office of the Ministry of Innovation and Technology in Hungary (TKP/ITM/NKFIH). Á. Kemény was supported by János Bolyai Research Scholarships of the Hungarian Academy of Sciences, and by the New National Excellence Program of the Ministry of Human Capacities (ÚNKP-19-4).

References

[1] G. Singh, Gastrointestinal complications of prescription and over-the-counter nonsteroidal anti-inflammatory drugs: a view from the ARAMIS database. Arthritis, Rheumatism, and Aging Medical Information System, Am. J. Ther. 7 (2000) 115–122, https://doi.org/10.1097/00045391-200007020-00008.

[2] L. Maiden, B. Thjodleifsson, A. Seigal, I.I. Bjarnason, D. Scott, S. Birgisson, et al., Long-term effects of nonsteroidal anti-inflammatory drugs and cyclooxygenase-2 selective agents on the small bowel: a cross-sectional capsule enteroscopy study, Clin. Gastroenterol. Hepatol. 5 (2007) 1040–1045, https://doi.org/10.1016/j.cgh.2007.04.031.

[3] J.L. Wallace, Mechanisms, prevention and clinical implications of nonsteroidal anti-inflammatory drug-enteropathy, World J. Gastroenterol. 19 (2013) 1861–1876, https://doi.org/10.3748/wjg.v19.i12.1861.

[4] K. Takeuchi, H. Satoh, NSAID-induced small intestinal damage–roles of various pathogenic factors, Digestion 91 (2015) 218–232, https://doi.org/10.1159/000374106.

[5] I. Bjarnason, C. Scarpignato, E. Holmgren, M. Olszewski, K.D. Rainsford, A. Lanas, Mechanisms of damage to the gastrointestinal tract from nonsteroidal anti-inflammatory drugs, Gastroenterology 154 (2018) 500–514, https://doi.org/10.1053/j.gastro.2017.10.049.

[6] J.M. Barrios, L.M. Lichtenberger, Role of biliary phosphatidylcholine in bile acid protection and NSAID injury of the ileal mucosa in rats, Gastroenterology 118 (2000) 1179–1186, https://doi.org/10.1016/S0016-5085(00)70371-4.

[7] M. Petruzzelli, A. Moschetta, W. Renooij, M.B. de Smet, G. Palasciano, P. Portincasa, et al., Indomethacin enhances bile salt detergent activity: relevance for NSAIDs-induced gastrointestinal mucosal injury, Dig. Dis. Sci. 51 (2006) 766–774, https://doi.org/10.1007/s10620-006-3204-1.

[8] R.W. Blackler, G. De Palma, A. Manko, G.J. Da Silva, K.L. Flannigan, P. Bercik, et al., Deciphering the pathogenesis of NSAID enteropathy using proton pump inhibitors and a hydrogen sulfide-releasing NSAID, Am. J. Physiol. Gastrointest. Liver Physiol. 308 (2015) G994–G1003, https://doi.org/10.1152/ajpgi.00066.2015.

[9] E.J. Dial, P.A. Dawson, L.M. Lichtenberger, In vitro evidence that phosphatidylcholine protects against indomethacin/bile acid-induced injury to cells, Am. J. Physiol. Gastrointest. Liver Physiol. 308 (2015) G217–G222, https://doi.org/10.1152/ajpgi.00322.2014.

[10] T. Yamada, M. Hoshino, T. Hayakawa, Y. Kamiya, H. Ohhara, K. Mizuno, et al., Bile secretion in rats with indomethacin-induced intestinal inflammation, Am. J. Physiol. 270 (1996) G804–G812, https://doi.org/10.1152/ajpgi.1996.270.5.G804.

[11] A. Uchida, T. Yamada, T. Hayakawa, M. Hoshino, Taurochenodeoxycholic acid ameliorates and ursodeoxycholic acid exacerbates small intestinal inflammation, Am. J. Physiol. 272 (1997) G1249–G1257, https://doi.org/10.1152/ajpgi.1997.272.5.G1249.

[12] A.F. Hofmann, The continuing importance of bile acids in liver and intestinal disease, Arch. Intern. Med. 159 (1999) 2647–2658, https://doi.org/10.1001/archinte.159.22.2647.

[13] L. Montenegro, G. Losurdo, R. Licinio, M. Zamparella, F. Giorgio, E. Ierardi, et al., Non steroidal anti-inflammatory drug induced damage on lower gastro-intestinal tract: is there an involvement of microbiota? Curr. Drug Saf. 9 (2014) 196–204, https://doi.org/10.2174/1574886309666140424143852.

[14] J.M. Ridlon, S.C. Harris, S. Bhowmik, D.J. Kang, P.B. Hylemon, Consequences of bile salt biotransformations by intestinal bacteria, Gut Microbes 7 (2016) 22–39, https://doi.org/10.1080/19490976.2015.1127483.

[15] T. Yang, T. Shu, G. Liu, H. Mei, X. Zhu, X. Huang, et al., Quantitative profiling of 19 bile acids in rat plasma, liver, bile and different intestinal section contents to investigate bile acid homeostasis and the application of temporal variation of endogenous bile acids, J. Steroid Biochem. Mol. Biol. 172 (2017) 69–78, https://doi.org/10.1016/j.jsbmb.2017.05.015.

[16] S.I. Sayin, A. Wahlström, J. Felin, S. Jäntti, H.U. Marschall, K. Bamberg, et al., Gut microbiota regulates bile acid metabolism by reducing the levels of tauro-beta-muricholic acid, a naturally occurring FXR antagonist, Cell Metab. 17 (2013) 225–235, https://doi.org/10.1016/j.cmet.2013.01.003.

[17] X. Zhou, L. Cao, C. Jiang, Y. Xie, X. Cheng, K.W. Krausz, et al., PPARα-UGT axis activation represses intestinal FXR-FGF15 feedback signalling and exacerbates experimental colitis, Nat. Commun. 5 (2014), https://doi.org/10.1038/ncomms5573.

[18] Z. Lu, Y. Lu, X. Wang, F. Wang, Y. Zhang, Activation of intestinal GR-FXR and PPARα-UGT signaling exacerbates ibuprofen-induced enteropathy in mice, Arch. Toxicol. 92 (2018) 1249–1265, https://doi.org/10.1007/s00204-017-2139-y.

[19] T.H. Kent, R.M. Cardelli, F.W. Stamler, Small intestinal ulcers and intestinal flora in rats given indomethacin, Am. J. Pathol. 54 (1969) 237–249.

[20] M. Uejima, T. Kinouchi, K. Kataoka, I. Hiraoka, Y. Ohnishi, Role of intestinal bacteria in ileal ulcer formation in rats treated with a nonsteroidal antiinflammatory drug, Microbiol. Immunol. 40 (1996) 553–560, https://doi.org/10.1111/j.1348-0421.1996.tb01108.x.

[21] T. Watanabe, H. Nishio, T. Tanigawa, H. Yamagami, H. Okazaki, K. Watanabe, et al., Probiotic Lactobacillus casei strain Shirota prevents indomethacin-induced small intestinal injury: involvement of lactic acid, Am. J. Physiol. Gastrointest. Liver Physiol. 297 (2009) G506–G513, https://doi.org/10.1152/ajpgi.90553.2008.

[22] E. Terán-Ventura, M. Aguilera, P. Vergara, V. Martínez, Specific changes of gut commensal microbiota and TLRs during indomethacin-induced acute intestinal inflammation in rats, J. Crohns Colitis 8 (2014) 1043–1054, https://doi.org/10.1016/j.crohns.2014.02.001.

[23] D. Maseda, J.P. Zackular, B. Trindade, L. Kirk, J.L. Roxas, L.M. Rogers, et al., Nonsteroidal anti-inflammatory drugs alter the microbiota and exacerbate clostridium difficile colitis while dysregulating the inflammatory response, mBio 10 (2019) e02282–e02318, https://doi.org/10.1128/mBio.02282-18.

[24] M.A.M. Rogers, D.M. Aronoff, The influence of non-steroidal anti-inflammatory drugs on the gut microbiome, Clin. Microbiol. Infect. 22 (2016) 178.e1–178.e9, https://doi.org/10.1016/j.cmi.2015.10.003.

[25] T. Watanabe, K. Higuchi, A. Kobata, H. Nishio, T. Tanigawa, M. Shiba, et al., Non-steroidal anti-inflammatory drug-induced small intestinal damage is Toll-like receptor 4 dependent, Gut 57 (2008) 181–187, https://doi.org/10.1136/gut.2007.125963.

[26] M. Begley, C.G. Gahan, C. Hill, The interaction between bacteria and bile, FEMS Microbiol. Rev. 29 (2005) 625–651, https://doi.org/10.1016/j.femsre.2004.09.003.

[27] P. Pavlidis, N. Powell, R.P. Vincent, D. Ehrlich, I. Bjarnason, B. Hayee, Systematic review: bile acids and intestinal inflammation-luminal aggressors or regulators of mucosal defence? Aliment. Pharmacol. Ther. 42 (2015) 802–817, https://doi.org/10.1111/apt.13333.

[28] D. Laukens, B.M. Brinkman, J. Raes, M. De Vos, P. Vandenabeele, Heterogeneity of the gut microbiome in mice: guidelines for optimizing experimental design, FEMS Microbiol. Rev. 40 (2016) 117–132, https://doi.org/10.1093/femsre/fuv036.

[29] D.A. Brodie, P.G. Cook, B.J. Bauer, G.E. Dagle, Indomethacin-induced intestinal lesions in the rat, Toxicol. Appl. Pharmacol. 17 (1970) 615–624, https://doi.org/10.1016/0041-008X(70)90036-0.

[30] X. Liang, K. Bittinger, X. Li, D.R. Abernethy, F.D. Bushman, G.A. FitzGerald, Bidirectional interactions between indomethacin and the murine intestinal microbiota, eLife 4 (2015) e08973, https://doi.org/10.7554/eLife.08973.

[31] P. Flecknell, Replacement, reduction and refinement, Altex 19 (2002) 73–78.

[32] S.J. Byun, T.J. Lim, Y.J. Lim, J.G. Seo, M.J. Chung, In vivo effects of s-pantoprazole, polaprenzinc, and probiotic blend on chronic small intestinal injury induced by indomethacin, Benef. Microbes 7 (2016) 731–737, https://doi.org/10.3920/BM2016.0029.

[33] S.B. László, B. Lázár, G.B. Brenner, A. Makkos, M. Balogh, M. Al-Khrasani, et al., Chronic treatment with rofecoxib but not ischemic preconditioning of the myocardium ameliorates early intestinal damage following cardiac ischemia/reperfusion injury in rats, Biochem. Pharmacol. 178 (2020) 114099, https://doi.org/10.1016/j.bcp.2020.114099.

[34] D.M. Heuman, Quantitative estimation of the hydrophilic-hydrophobic balance of mixed bile salt solutions, J. Lipid Res. 30 (1989) 719–730, https://doi.org/10.1016/S0022-2275(20)38331-0.

[35] L.K. Stenman, R. Holma, R. Forsgård, H. Gylling, R. Korpela, Higher fecal bile acid hydrophobicity is associated with exacerbation of dextran sodium sulfate colitis in mice, J. Nutr. 143 (2013) 1691–1697, https://doi.org/10.3945/jn.113.180810.

[36] M. Poša, Heuman indices of hydrophobicity of bile acids and their comparison with a newly developed and conventional molecular descriptors, Biochimie 97 (2014) 28–38, https://doi.org/10.1016/j.biochi.2013.09.010.

[37] B. Lázár, G. Brenner, A. Makkos, M. Balogh, S. László, M. Al-Khrasani, et al., Lack of small intestinal dysbiosis following long-term selective inhibition of cyclooxygenase-2 by rofecoxib in the rat, Cells 8 (2019) 251, https://doi.org/10.3390/cells8030251.

[38] B. Mansour, Á. Monyók, N. Makra, M. Gajdács, I. Vadnay, B. Ligeti, et al., Bladder cancer-related microbiota: examining differences in urine and tissue samples, Sci. Rep. 10 (2020) 11042, https://doi.org/10.1038/s41598-020-67443-2.

[39] P. Ewels, M. Magnusson, S. Lundin, M. Käller, MultiQC: summarize analysis results for multiple tools and samples in a single report, Bioinformatics 32 (2016) 3047–3048, https://doi.org/10.1093/bioinformatics/btw354.

[40] A.M. Bolger, M. Lohse, B. Usadel, Trimmomatic: a flexible trimmer for Illumina sequence data, Bioinformatics 30 (15) (2014) 2114–2120, https://doi.org/10.1093/bioinformatics/btu170.

[41] C. Quast, E. Pruesse, P. Yilmaz, J. Gerken, T. Schweer, P. Yarza, et al., The SILVA ribosomal RNA gene database project: improved data processing and web-based tools, Nucleic Acids Res. 41 (2013) D590–D596, https://doi.org/10.1093/nar/gks1219.

[42] D.E. Wood, S.L. Salzberg, Kraken: ultrafast metagenomic sequence classification using exact alignments, Genome Biol. 15 (2014) R46, https://doi.org/10.1186/gb-2014-15-3-r46.

[43] F.P. Breitwieser, J. Lu, S.L. Salzberg, A review of methods and databases for metagenomic classification and assembly, Brief Bioinform. 20 (2019) 1125–1136, https://doi.org/10.1093/bib/bbx120.

[44] S. Mandal, W. Van Treuren, R.A. White, M. Eggesbø, R. Knight, S.D. Peddada, Analysis of composition of microbiomes: a novel method for studying microbial composition, Microb. Ecol. Health Dis. 26 (2015) 27663, https://doi.org/10.3402/mehd.v26.27663.

[45] Y. Benjamini, Y. Hochberg, Controlling the false discovery rate: a practical and powerful approach to multiple testing, J. R. Stat. Soc. Ser. B: Stat. Methodol. 57 (1995) 289–300, https://doi.org/10.1111/j.2517-6161.1995.tb02031.x.

[46] R Core Team, A Language and Environment for Statistical Computing, R Foundation for Statistical Computing, Vienna, Austria, 2018. URL: http://www.R-project.org/.

[47] A. Higashimori, T. Watanabe, Y. Nadatani, S. Takeda, K. Otani, T. Tanigawa, et al., Mechanisms of NLRP3 inflammasome activation and its role in NSAID-induced enteropathy, Mucosal Immunol. 9 (2016) 659–668, https://doi.org/10.1038/mi.2015.89.

[48] Y.M. Han, J.M. Park, J.X. Kang, J.Y. Cha, H.J. Lee, M. Jeong, et al., Mitigation of indomethacin-induced gastrointestinal damages in fat-1 transgenic mice via gatekeeper action of ω-3-polyunsaturated fatty acids, Sci. Rep. 6 (2016) 33992, https://doi.org/10.1038/srep33992.

[49] P. Hegyi, J. Maléth, J.R. Walters, A.F. Hofmann, S.J. Keely, Guts and gall: bile acids in regulation of intestinal epithelial function in health and disease, Physiol. Rev. 98 (2018) 1983–2023, https://doi.org/10.1152/physrev.00054.2017.

[50] M. Craven, C.E. Egan, S.E. Dowd, S.P. McDonough, B. Dogan, E.Y. Denkers, et al., Inflammation drives dysbiosis and bacterial invasion in murine models of ileal Crohn's disease, PLoS One 7 (2012) e41594, https://doi.org/10.1371/journal.pone.0041594.

[51] Á. Tóth, I. Damjanova, E. Puskás, L. Jánvári, M. Farkas, A. Dobák, et al., Emergence of a colistin-resistant KPC-2-producing Klebsiella pneumoniae ST258 clone in Hungary, Eur. J. Clin. Microbiol. Infect. Dis. 29 (2010) 765–769, https://doi.org/10.1007/s10096-010-0921-3.

[52] G. Martin, S. Kolida, J.R. Marchesi, E. Want, J.E. Sidaway, J.R. Swann, In vitro modeling of bile acid processing by the human fecal microbiota, Front. Microbiol. 9 (2018) 1153, https://doi.org/10.3389/fmicb.2018.01153.
[53] S. Kurata, T. Nakashima, T. Osaki, N. Uematsu, M. Shibamori, K. Sakurai, et al., Rebamipide protects small intestinal mucosal injuries caused by indomethacin by modulating intestinal microbiota and the gene expression in intestinal mucosa in a rat model, J. Clin. Biochem. Nutr. 56 (2015) 20–27.
[54] N. Dikopoulos, R.M. Schmid, M. Bachem, K. Buttenschoen, G. Adler, J.Y. Chiang, et al., Bile synthesis in rat models of inflammatory bowel diseases, Eur. J. Clin. Invest. 37 (3) (2007) 222–230, https://doi.org/10.1111/j.1365-2362.2007.01779.x.
[55] M. Makishima, A.Y. Okamoto, J.J. Repa, H. Tu, R.M. Learned, A. Luk, et al., Identification of a nuclear receptor for bile acids, Science 284 (1999) 1362–1365, https://doi.org/10.1126/science.284.5418.1362.
[56] F. Chen, L. MA, R.B. Sartor, F. Li, H. Xiong, A.Q. Sun, et al., Inflammatory-mediated repression of the rat ileal sodium-dependent bile acid transporter by c-fos nuclear translocation, Gastroenterology 123 (2002) 2005–2016, https://doi.org/10.1053/gast.2002.37055.
[57] W.A. Alrefai, R.K. Gill, Bile acid transporters: structure, function, regulation and pathophysiological implications, Pharm. Res. 24 (2007) 1803–1823, https://doi.org/10.1007/s11095-007-9289-1.
[58] F. Rowan, N.G. Docherty, M. Murphy, B. Murphy, J. Calvin Coffey, P.R. O'Connell, Desulfovibrio bacterial species are increased in ulcerative colitis, Dis. Colon Rectum 53 (2010) 1530–1536, https://doi.org/10.1007/DCR.0b013e3181f1e620.
[59] S. Devkota, Y. Wang, M.W. Musch, V. Leone, H. Fehlner-Peach, A. Nadimpalli, et al., Dietary-fat-induced taurocholic acid promotes pathobiont expansion and colitis in Il10−/− mice, Nature 487 (2012) 104–108, https://doi.org/10.1038/nature11225.
[60] L.R. Lopetuso, F. Scaldaferri, V. Petito, A. Gasbarrini, Commensal Clostridia: leading players in the maintenance of gut homeostasis, Gut Pathog. 5 (2013) 23, https://doi.org/10.1186/1757-4749-5-23.
[61] J.L. Wallace, S. Syer, E. Denou, G. de Palma, L. Vong, W. McKnight, et al., Proton pump inhibitors exacerbate NSAID-induced small intestinal injury by inducing dysbiosis, Gastroenterology 141 (2011) 1314–1322.e5, https://doi.org/10.1053/j.gastro.2011.06.075.
[62] B.S. Scales, R.P. Dickson, G.B. Huffnagle, A tale of two sites: how inflammation can reshape the microbiomes of the gut and lungs, J. Leukoc. Biol. 100 (2016) 943–950, https://doi.org/10.1189/jlb.3MR0316-106R.
[63] K. Shindo, K. Fukushima, Deconjugation of bile acids by human intestinal bacteria, Gastroenterol. Jpn. 11 (1976) 167–174, https://doi.org/10.1007/BF02777700.
[64] M.Y. Zeng, N. Inohara, G. Nuñez, Mechanisms of inflammation-driven bacterial dysbiosis in the gut, Mucosal Immunol. 10 (2017) 18–26, https://doi.org/10.1038/mi.2016.75.
[65] S.H. Duncan, P. Louis, J.M. Thomson, H.J. Flint, The role of pH in determining the species composition of the human colonic microbiota, Environ. Microbiol. 11 (2009) 2112–2122, https://doi.org/10.1111/j.1462-2920.2009.01931.x.
[66] D.P. Singh, S.P. Borse, M. Nivsarkar, A novel model for NSAID induced gastroenteropathy in rats, J. Pharmacol. Toxicol. Methods 78 (2016) 66–75, https://doi.org/10.1016/j.vascn.2015.11.008.
[67] P. Zimmermann, N. Curtis, Antimicrobial effects of antipyretics, Antimicrob. Agents Chemother. 61 (2017) e02268–e2316, https://doi.org/10.1128/AAC.02268-16.
[68] R. Colucci, C. Pellegrini, M. Fornai, E. Tirotta, L. Antonioli, C. Renzulli, et al., Pathophysiology of NSAID-associated intestinal lesions in the rat: luminal bacteria and mucosal inflammation as targets for prevention, Front. Pharmacol. 9 (2018), https://doi.org/10.3389/fphar.2018.01340.s003.